Chapter 10

Thermoregulation

Nigel J. Blake[1], Adam F. Parlin[2], Iain Cumming[3], James P. Gibbs[4,5], Glenn J. Tattersall[6], Daniel E. Warren[7], Freddy Cabrera[8], Jose Haro[8], Jack Norys[7], Randall James[7] and Stephen Blake[7,8,9,10]

[1]Nigel Blake Engineering Consulting Limited, Richmond, United Kingdom, [2]Department of Biology, University of Cincinnati, Cincinnati, OH, United States, [3]Department of Chemical Engineering, Loughborough University, Loughborough, United Kingdom, [4]State University of New York College of Environmental Science and Forestry, Syracuse, NY, United States, [5]Galapagos Conservancy, Fairfax, VA, United States, [6]Biological Sciences, Brock University, St. Catharines, ON, Canada, [7]Department of Biology, Saint Louis University, St. Louis, MO, United States, [8]Charles Darwin Foundation, Puerto Ayora, Galapagos, Ecuador, [9]Department of Migration, Max Planck Institute of Animal Behavior, Radolfzell, Germany, [10]WildCare Institute, Saint Louis Zoo, Saint Louis, MO, United States

Chapter outline

Introduction

Galapagos tortoises are ectotherms and as such generate insufficient metabolic heat to regulate their internal temperature. Local environmental conditions interact with intrinsic characteristics of ectotherms such as body size, morphology, and activity to determine internal (core) temperature regimes (Shine 2005). Internal temperature directly influences metabolic rate and physiological performance, and so failure to maintain core body temperature within optimal or tolerable limits will have negative consequences for the energy balance and body functions of organisms such as digestion, movement, growth, and immune responses (Angilletta 2001; O'Connor 1999; Wikelski and Romero 2003; Zimmerman *et al.* 1994). Low core temperatures will lead to slow and inefficient digestion and inhibit tissue growth and repair and gamete maturation. High core temperatures can cause thermal stress, leading to tissue damage. High or low temperature extremes may cause death.

Body size plays a major role in thermoregulation in ectotherms because it is a primary determinant of thermal inertia, the rate at which the temperature of a body approaches that of its surroundings. Larger objects gain and lose heat more slowly than smaller ones. This is particularly germane to Galapagos tortoises, which are unique among vertebrates in their huge variation in body size, ranging over four orders of magnitude on many islands, from tiny 0.05-kg hatchlings to c. 300-kg adults (Fig. 10.1), with important implications for temperature regulation. Small tortoises have low thermal inertia and therefore will track ambient temperature more closely compared to larger tortoises, and thus potentially experience greater variation in core temperature. Small tortoises may need to use behavioral thermoregulatory mechanisms more frequently to maintain acceptable internal temperature and may require different local conditions compared to larger tortoises, such as variable microhabitats with different thermal properties.

Galapagos Giant Tortoises. DOI: https://doi.org/10.1016/B978-0-12-817554-5.00015-0

FIGURE 10.1 Galapagos tortoise body mass ranges from 50 g (top) to 300 kg (bottom), or four orders of magnitude, which means that there is enormous variation in rates of heat transfer between the smallest and largest tortoises. Such a size range makes Galapagos tortoises ideal subjects to study the effects of body size on physiology and ecology in biology more generally. *Photos: Christian Zeigler (top), Stephen Blake (bottom).*

Giant tortoises are continually faced with a series of behavioral trade-offs that influence immediate thermal balances and energy budgets (Fig. 10.2). Behavioral thermoregulation (e.g., basking, remaining in shade, or migrating out of suboptimal thermal conditions) can be considered an opportunity cost because of the reduced time available for foraging, moving, or other behaviors (Angilletta 2009). These short-term decisions scale up over time to have consequences for body condition, health, and reproductive output, which further scale up to adaptive responses to selective pressure and ultimately the evolutionary trajectories of populations and species.

The trade-off between behavioral thermoregulation and other activities has been documented among giant tortoises on Aldabra Atoll in the Seychelles. On Aldabra, subadult and adult giant tortoises (*Aldabrachelys gigantea*) migrate between inland areas with moderate food availability and abundant shade, and coastal areas with abundant nutritious forage but little shade (Swingland 1977; Swingland *et al.* 1989). Swingland and Frazier (1980:611–615) showed that tortoises face a conflict of life and death proportions when deciding how much time to invest in foraging in the open versus seeking shade. Body size determines the distribution of tortoises in these habitats, with larger tortoises ranging farther from the nearest shade. Tortoises attempting to maximize their food intake must judge precisely when to stop feeding and move into shade, because failure to do so may result in death due to overheating. Larger tortoises have the additional constraint of continuing to warm even after finding shade due to their thermal inertia and can die of overheating hours after leaving direct sun. Small tortoises must remain close to cover because they heat up much more rapidly but also cool down more quickly in the shade.

The Galapagos Archipelago has more variable terrestrial environments than Aldabra due to much greater topographical variation and its location in the equatorial eastern Pacific (Colinvaux 1984:55–69; Conroy *et al.* 2008; Restrepo *et al.* 2012). Interactions among island location, island topography, and seasonal shifts in predominant ocean currents, which largely determine climate conditions on the small landmasses of Galapagos, combine to create diverse local conditions in time and space (Trueman and d'Ozouville 2010) and a unique climate with implications for ectothermic reptiles. Compared to the rest of the Tropics, Galapagos annual temperatures are slightly below average, annual fluctuation between high and low temperatures are very low (only 5°C–7°C), daily fluctuations in temperature are modest, and annual precipitation is low although the *garúa* phenomenon in Galapagos—mist that occurs at mid-elevations during the cool, dry season (June–December)—ensures that some precipitation persists during the dry season in Galapagos, whereas most other tropical regions typically receive no precipitation during their dry seasons (Chapter 14: Habitats).

These abiotic conditions drive vegetation patterns that impose both coarse- and fine-grained structure on local air temperature and present Galapagos tortoises with contrasting thermal environments (Fig. 10.3). Soil temperature in full sun may be several tens of degrees hotter than the soil 3 m away under the cover of trees or other vegetation. Different species of Galapagos tortoises distributed throughout the Archipelago encounter a wide range of temperature conditions, from hot, arid islands such as Española and Pinzón, to cool, moist uplands on Isabela, Santa Cruz, and other islands with humid highlands. Among migratory species of Galapagos tortoises (Chapter 13: Movement Ecology), the same individual may encounter dramatically different conditions during annual migrations (Fig. 10.3; Blake *et al.* 2013). Indeed, while tortoise migration is driven largely by spatiotemporal variability in forage quality, the thermal environment also significantly

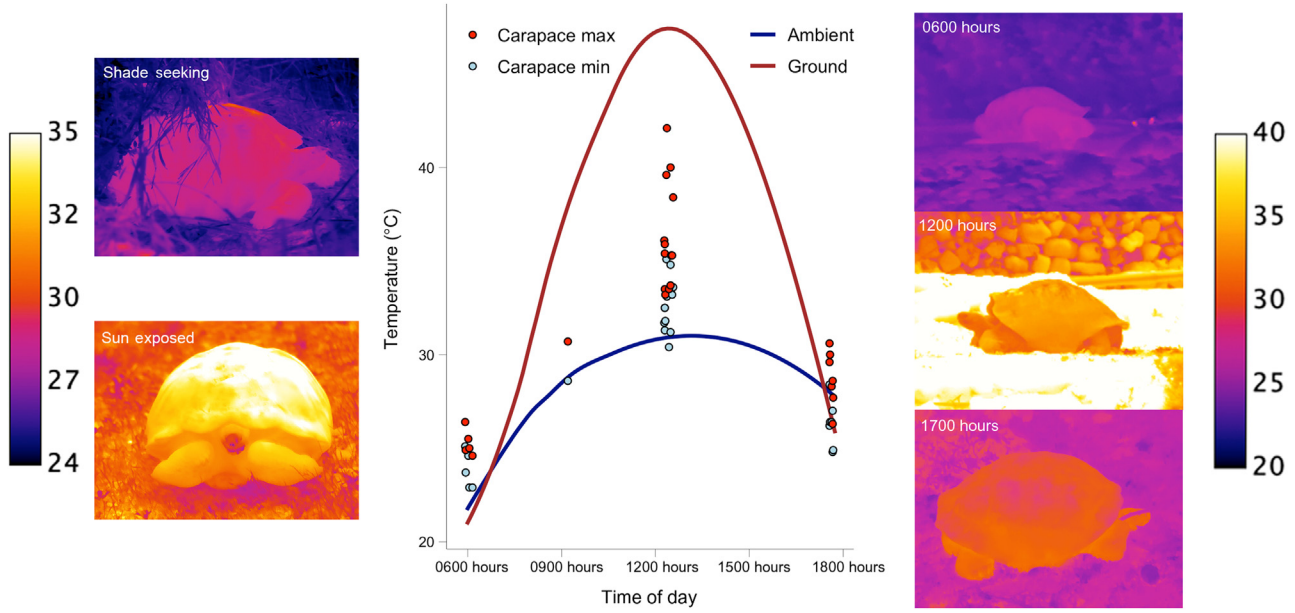

FIGURE 10.2 Giant tortoises are continually faced with a series of behavioral trade-offs that influence immediate thermal balances and energy budgets. Here infrared images captured in April–May 2013 depict wild tortoises (left side) exhibiting shade-seeking (28.8°C) and sun-exposed (35.0°C) behaviors, as well as captive tortoises (right side) during different times of the day: 0600 (25.9°C), 1200 (33.5°C), and 1700 hours (29.5°C). The center image depicts the minimum and maximum carapace temperatures recorded from the captive tortoises during the same time, bounded by ambient and ground temperatures derived from smoothed averages from the same field site over the same measurement period. Temperature scales correspond to the respective, adjacent images.

FIGURE 10.3 At a habitat scale, a Western Santa Cruz Island tortoise (*Chelonoidis porteri*) in the highlands in September can select either full sun (top left) or heavy shade (top right) within the heterogeneous vegetation mosaic of open pastures and dense tree cover. At a landscape scale, a migratory Western Santa Cruz tortoise in the highlands during the cool dry season (lower left) and in the lowlands during the hot wet season (lower right); the tortoise is in the coolest location during the coolest season in the upland phase of the migration, and the hottest location in the hottest season during the lowland phase of the migration. *Photos: Stephen Blake.*

contributes to the energy budget of tortoises and must be accounted for in modeling the cost–benefit analysis of migratory behavior relative to other movement strategies (Yackulic *et al.* 2017; Chapter 13: Movement Ecology).

Galapagos tortoises are, like their Aldabra Atoll counterparts, under strong selective pressure to optimize their physiological performance across a range of environmental conditions, requiring tortoise species on different islands and volcanoes to adapt to strongly varying local

conditions. Adaptation can be manifested over short time scales (minutes, hours, and days) via behavioral decisions that determine activity budgets (Harlow *et al.* 2010; Kearney *et al.* 2009) including basking in the sun with limbs extended to warm up after cool nights, seeking shade and becoming inactive during the middle of the day to shed heat, or wallowing in pools at night to reduce cooling. Tortoises in variable environments require habitats that offer a variety of microclimates in which they can alter their core temperature. Insufficient shade may have catastrophic consequences (Swingland and Frazier 1980:611–615). In contrast, extensive dense cloud cover may render tortoises unable to warm their core temperature during the long cool seasons in the highlands. These short-term behaviors and their consequences in response to temperature will scale up to evolutionary responses at the population level (Ricklefs and Wikelski 2002). For example, along with ecological and social selective pressures (Fritts 1984), adaptations to local thermal conditions may, at least in part, explain why saddleback tortoises occur on hot, dry islands. Morphological characteristics of saddleback tortoises, including large surface areas of skin, and thin, elevated carapaces, allow rapid heat loss (Chapter 8: Morphology). In contrast, dome tortoises, with thick shells that cover most of the body, occur on islands with cool humid highlands where heat conservation may be advantageous.

Thermoregulation in Galapagos tortoises is germane at a time of unprecedented global climate change (IPCC 2014; Nolan *et al.* 2018) and accelerating impacts of anthropogenic change on land use and ecosystems on Galapagos (Chapter 16: Climate Change). Since the arrival of humans, vegetation structure has dramatically changed (Restrepo *et al.* 2012) throughout the Archipelago due to actions of invasive herbivorous mammals (Chapter 19: Invasive Species) and habitat conversion on settled islands (Khatun 2018; Walsh and Mena 2016; Watson *et al.* 2010). These modifications of habitat quality include changes in the thermal landscape for giant tortoises (Fischer and Lindenmayer 2007; Tuff *et al.* 2016). Understanding how current and future conditions will influence local environments for Galapagos tortoises and their behavioral repertoire for thermoregulation is important for predicting the impacts of climate change and to guide management to mitigate negative consequences.

Understanding thermoregulation in Galapagos tortoises

Thermal ecology is a rapidly expanding field that seeks to understand the dynamic nature of how thermal energy flows between organisms and their environment; how an organism regulates these flows; and the consequences on their energy balance, physiology, behavior, ecosystem interactions, and fitness (Ihlow *et al.* 2012; Kearney and Porter 2017). Heat, or the total energy of all the molecular motion inside an object, in this case, a giant tortoise, is transferred through four fundamental physical processes: (1) conduction—the direct transfer of heat between solid bodies in contact with each other; (2) convection—heat exchange between fluids (liquid or gas) or from solids to fluids; (3) radiation—transfer of heat energy by photons; and (4) evaporative water loss—heat loss during phase change from liquid to gas. One method for visualizing heat balance is by applying a thermal circuit diagram (e.g., Bakken 1976) to map the routes of heat flux from different sources. These routes include absorbance of radiation from the atmosphere or scattered solar radiation, radiative heat loss to the environment, convective heat transfer with the ground, and evaporative water loss between the tortoise and the environment (Fig. 10.4). Mathematical models in the past have focused on calculating the temperature at the surface of the ectotherm and then the transfer of heat to the core of the body (O'Connor 2000; Spotila *et al.* 1973; Zimmerman *et al.* 1994). However, the carapace of the tortoise adds an extra layer of complexity (O'Connor *et al.* 2000). Compared to the dermal layer of nonchelonian ectotherms, the carapace of tortoises exhibits different thermal properties including specific heat capacity and thermal conductance (O'Connor *et al.* 2000). Such differences need to be considered when calculating the heat balance of a Galapagos tortoise. Moreover, published accounts of heat balance in ectotherms have not included the full complement of heat-balance pathways nor have they, in some cases, included enough detail in documenting the underlying mechanism of each of the balances to quantify each element of each balance (Fei *et al.* 2012; Kearney and Porter 2017; O'Connor 1999; Spotila *et al.* 1973; Turner and Tracy 1985).

Under consideration of these issues, a mathematical model was developed to estimate heat balance in Galapagos tortoises. The tortoise's complex shape was simplified as a hemisphere, with no account made of the head, neck, limbs, or tail in this first iteration. The plastron was split into two sections, one area touching the ground and the other occupying an air gap separating it from the ground. Heat entered or left the tortoise via conduction through the carapace and plastron as well as via convection from breathing and surface evaporation. Metabolic heat was generated internally by the tortoise. Whereas tortoises can control body heat by adjusting blood flow and exposure of limbs, neck, and head, this aspect of thermoregulation was not considered such that body temperature was assumed to be the same throughout the tortoise and determined by the heat capacity of the internal tissue mass within the animal's body core.

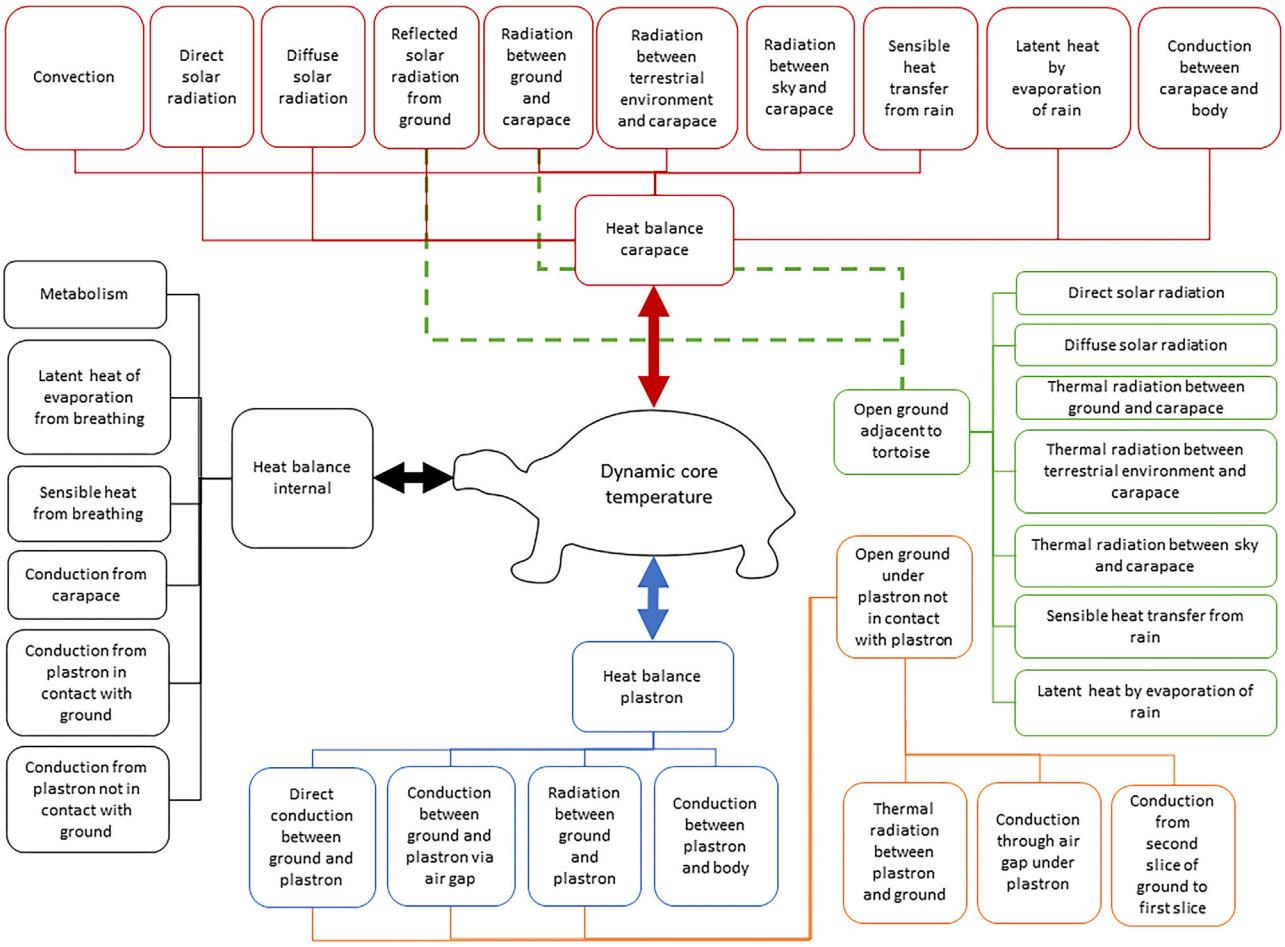

FIGURE 10.4 Heat flows considered in the model of Galapagos tortoise thermoregulation.

Based on these interacting components, the model predicts the internal (core) and external (carapace and plastron) temperatures for a Galapagos tortoise of a given size by solving a series of seven heat balances:

1. the tortoise's carapace;
2. the section of the tortoise's plastron in direct contact with the ground;
3. the section of the tortoise's plastron not in direct contact with the ground;
4. the tortoise's internal tissue mass;
5. the open ground adjacent to the tortoise;
6. the ground under and in contact with the tortoise's plastron, and
7. the ground under but not in contact with the tortoise's plastron.

Predictions were made by considering major sources of heat exchange, the primary one being radiation. During daylight hours most of the heat is derived from direct and reflected solar radiation. The model considered variation of sun intensity throughout the year, sun elevation, scattered radiation, and cloud cover. At night the tortoise radiated heat to the sky. Infrared heat gain and loss between the tortoise and surrounding ground vegetation during night and day were also included. The velocity of the wind blowing over the tortoise and air temperature were included as important sources of heating and cooling via convective heat transfer. Both wind speed and air temperature follow sinusoidal profiles in the Galapagos Islands (S. Blake, unpubl. data) fitted via general sinusoidal equations throughout the diurnal cycle by setting the values at 0700 and 2100 hours. In addition, rain falling on and wetting the tortoise's surface and the surrounding ground was considered.

Mathematical equations were then developed to determine heat fluxes due to radiation, conduction through the carapace, plastron, and ground, as well as forced convection from air and water flow over the carapace mediated by wetness of the tortoise's surface, based on two literature sources, one describing heat and mass transfer as well as that associated with water flow over the carapace (Bird *et al.* 1960) and the second providing standard values of view factors, that is, proportion of the radiation leaving one surface that strikes another (Howell 2019). The elevation

of the sun was calculated from the position of the sun (https://en.wikipedia.org/wiki/Position_of_the_Sun) and radiation was partitioned by that arriving directly and by scattering from the sun (Wang 2001).

The final sources of heat exchange considered were breathing and heat generated internally by a tortoise. The heat exchange from evaporation or condensation in the process of breathing was calculated from the metabolic rate and an estimated change in oxygen concentration between inhalation and exhalation of air, which allowed the volume of air breathed to be calculated. Internal heat generation was estimated from the metabolic rate of a tortoise as given by Andrews and Pough (1985).

Using this information, each of the seven heat balances was integrated numerically over a series of small time intervals, with all temperatures and heat fluxes updated after each time interval. The temperature profile into the ground and through the plastron, where the plastron was in contact with the ground, was solved using the one-dimensional (1-D) partial differential heat conduction equation in the form of a difference equation. For the area where the plastron was not in contact with the ground, this partial differential equation was only applied to the ground. The solution to the heat balances and their numerical integration are described in detail in Appendix 10.1.

Balancing heat load in the thermal environment of Galapagos

Estimates of the preferred internal temperature range for Galapagos tortoises are presented as bounded by core temperature thresholds, an upper thermal threshold (UTT) and a lower thermal threshold (LTT), above and below which tortoises become inactive due to hostile or suboptimal conditions. These values enabled: (1) consistent comparative reference points to interpret model outputs, and (2) hypotheses to be generated about how tortoises thermoregulate under varying extrinsic and intrinsic conditions. The UTT was estimated at 33°C, and LTT at 25°C, based on unpublished data collected from small temperature loggers (iButtons, DS1922L, Maxim Integrated Products, San Jose, CA 95134, United States) fed to four adult Galapagos tortoises housed in captivity at 10 m elevation on Santa Cruz Island. Over 37 days, from August to October 2012, mean maximum and minimum internal temperatures were 25.8°C (±0.87) and 31.2°C (±1.69). As context, Aldabra giant tortoises rarely survive if body temperature exceeds 36°C for an extended period of time (Swingland and Frazier 1980:611–615; I. Swingland, pers. comm.). These thermal thresholds were also reflected in measurements taken (also with ingested iButtons) by Falcón *et al.* (2018), who recorded mean minimum and maximum internal temperatures of 26.1°C and 34.5°C for adult Aldabra giant tortoises.

The model (Fig. 10.4; Appendix 10.1) can clarify the complexities of thermoregulation faced by giant tortoises in Galapagos. Consider western Santa Cruz Island tortoises of different size classes at 10-m elevation in September under identical input conditions: tortoise inactive, no shade, no close vegetation, and no rain (Fig. 10.5). September is the coolest month of the year and 10 m is the lowest elevation of the tortoise range considered here. The enormous difference in temperature between ambient (shade) and ground, even at the coolest time of the year, is striking. Modeled maximum ambient temperature was 24°C, yet ground temperature in full sunlight attained a maximum of 75.3°C at 12:14 p.m. Minimum daily ambient temperature was 19.3°C, with carapace surface temperature dropping below this to 16.4°C by 6 a.m. To avoid overheating, a tortoise at 10-m elevation in September should seek shade for much of the day and seek cover at night to minimize excessive cooling to the sky.

Two trends regarding core and shell temperature are obvious but nevertheless noteworthy. First, as tortoise body size increases, the lag between core and shell temperature increases due to the thermal mass of larger tortoises. Second, the range of body temperature decreases as body size increases for the same reason. To illustrate, the maximum and minimum core temperatures of a 2-kg tortoise are 49.1°C and 17.4°C, while those for a 200-kg tortoise are 41.9°C and 30.7°C, respectively. Although both maxima would be lethal, the smaller predicted range allows larger tortoises to tolerate fluctuations in temperatures through the day more effectively than small tortoises and therefore larger

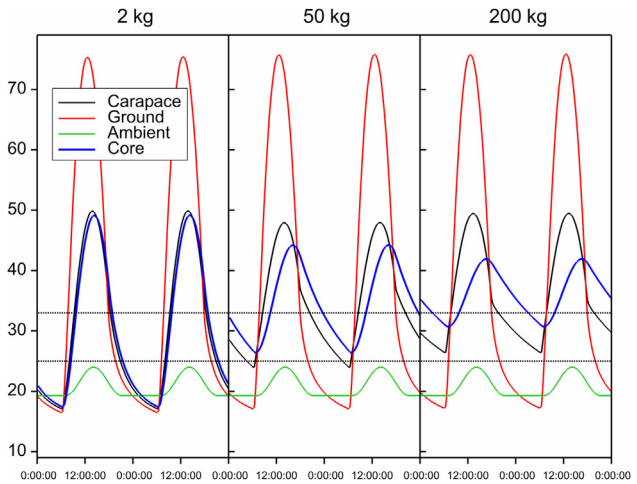

FIGURE 10.5 Estimates of four temperature profiles—ambient (T_a), open ground (T_o), carapace (T_c), and core (T_b)—for western Santa Cruz Island tortoises of different body mass at 10 m elevation, inactive, in the open, with no rain, no wind, and no close vegetation in September. The horizontal dashed lines represent estimated thermal thresholds for core temperature (LTT and UTT). Tortoises of all body sizes overheat, and the smaller tortoises are unable to maintain core temperatures above LTT at night. *LTT*, Lower thermal threshold; *UTT*, upper thermal threshold.

tortoises require less thermoregulatory behavior to maintain a more stable body temperature.

Without behavioral thermoregulation, tortoises of all size classes would be unable to remain within core temperature thresholds and would overheat to dangerous levels. The core temperature of a 2-kg tortoise is predicted to exceed UTT at 9:34 a.m., with only 16% of the day within core temperature thresholds. Even a 200-kg tortoise remains within core temperature thresholds for just 28% of the day. The 2-kg tortoise is also vulnerable to excessively low internal temperatures, spending 46% of its time below LTT.

Ground-truthing the model

The model was conceived and built by chemical engineer N.J. Blake (lead author) on a laptop computer in Richmond, Surrey, United Kingdom, far from sight of a Galapagos tortoise. In the model, local conditions, heat transfer pathways and their magnitudes, and the equations that describe them are all technically defensible (Appendix 10.1); nevertheless, a modeled core temperature of a hypothetical tortoise versus the core temperature of an actual tortoise wandering somewhere on the slopes of a volcano in Galapagos are two different things.

To ground-truth the model using empirical data collected on local ambient conditions and core temperatures of living tortoises, a field experiment was conducted in July 2019. Two tortoises, both adult males living in the highlands of Santa Cruz Island at 350-m elevation, were selected for the trial. The tortoises were fed iButtons programmed to collect internal temperature (to the nearest 0.5°C, every 15 minutes; Fig. 10.6). Each tortoise was also fitted

FIGURE 10.6 Steps involved in deploying an iButton temperature logger into the digestive tract of a Galapagos tortoise to record core temperature at 15-min intervals over a period of weeks. The iButton was glued to a VHF radio transmitter and hidden in a piece of banana, which was readily consumed by the tortoise. The iButton and radio were retrieved in a pile of tortoise dung following passage through the digestive tract, and the temperature data downloaded. *Photos: Stephen Blake.*

with a GPS unit for relocation. To relocate the iButtons after they were defecated, a small (6 g) radio receiver (RI 2B, Holohil, Carp, Ontario, Canada), minus its antenna, was glued to each one. To facilitate the tortoise ingesting the iButton with the radio transmitter, it was placed inside a piece of banana and offered to the tortoise on the end of a stick. Each tortoise readily ate the banana and swallowed the iButton-radio combination. Devices were successfully retrieved after defecation (Fig. 10.6).

Daily tracking of each tortoise was initiated at 7 a.m. and continued to 4 p.m. The following data were recorded every 15 minutes: tortoise activity, distance from nearest vegetation, distance from the nearest vegetation in line of sight to the sun, tortoise in open or shade, substrate under the tortoise, vegetation height, cloud cover, cloud type, clarity of sky, air temperature, wind speed, and humidity at the tortoise (collected using a handheld Kestrel 3000 Pocket Wind Meter, Kestrel Instruments, Boothwyn, PA 19061, United States), ambient temperature (to the nearest 0.5°C using an iButton inside a weather station housing), and precipitation strength (recorded as none, very light, light, moderate, heavy). These measurements reflected variable definitions in the model (Appendix 10.1). Environmental data and tortoise behavior data were not collected at night, as the location of the tortoises changed minimally after 4 p.m. as indicated by the GPS relocations.

Input data for the model were generated for each day from: (1) the maximum and minimum ambient temperature recorded, and (2) maximum, minimum, and average of environmental and tortoise behavior data as appropriate. For analysis, one tortoise was eliminated because he relocated into woodland c. 0.8 km from his original location, and his behavior was not conducive to the model inputs (he spent long hours in a muddy wallow and at times frequently moved in and out of partial shade). Future versions of the model will take such behaviors into account; the purpose here was to validate the model using field data consistent with the model input constraints. The tortoise ultimately serving as the trial subject was a moderately large male with a body radius of 0.4 m.

Congruence was remarkably high between what the model predicted and what the tortoise experienced (Fig. 10.7). The average and maximum difference between empirical and modeled ambient temperature over the 4 days were 0.0°C and 1.6°C, respectively, and the coefficient of variation of the difference was 0.57. Likewise, the average and maximum difference between actual and predicted core temperatures were 0.6°C and 2.4°C, respectively, with the coefficient of variation of the difference 0.14.

Given that the model is a first attempt built from scratch and developed from first principles, the level of predictive power is outstanding. Whereas more extensive field trials will allow iterative improvements

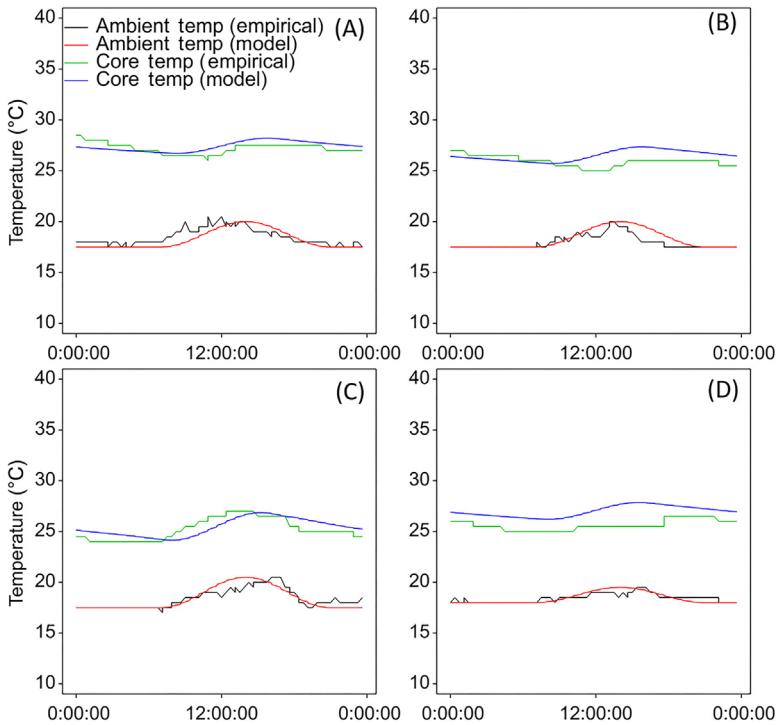

FIGURE 10.7 Comparisons of modelled ambient and core temperature (Fig. 10.6) compared to empirical measurements from an iButton temperature logger in the digestive tract of a Galapagos tortoise in the field over four consecutive days (panels A–D represent Aug 18–21, 2019, respectively).

to the model, the field trial demonstrated the utility of the model to investigate the role of environment, body size, and behavioral thermoregulation on temperature homeostasis of Galapagos tortoises.

Thermoregulation and Galapagos tortoise ecology

Based on successful field validation (Fig. 10.7), the predictive tool was used to evaluate the impact of five, real-world ecological scenarios for tortoise thermal ecology, including:

1. the effect of thermoregulatory behavior on core temperatures of Galapagos tortoises;
2. the distribution of tortoises by body size along an elevation gradient;
3. the ability of large versus small tortoises to maintain their core temperatures within thermal limits at the lowest elevation during the hottest month on Santa Cruz Island;
4. the impact of a 2°C increase in ambient temperature and a reduced cloud cover from plausible climate change scenarios (Zelinka *et al.* 2020) during the hottest month at the lowest elevation on Santa Cruz Island, and
5. the effect of shading by invasive Cuban cedar (*Cedrela odorata*) in the highlands of Santa Cruz.

Effect of thermoregulatory behaviors on core temperature

The effects of giant tortoise behaviors associated with thermoregulation on core temperature of a 200-kg Santa Cruz Island tortoise are compared at the coolest elevation regularly attained by tortoises during the coolest month of the year, that is, at an elevation of 400 m in September, which represents typical conditions at the destination of the upland migration (Blake *et al.* 2013; Yackulic *et al.* 2017; Chapter 13: Movement Ecology). Behaviors include an inactive tortoise in open habitat, in the wind, far from vegetation (50 m from vegetation that is 5 m in height), and with no rain. Compared to this is a tortoise either (1) sheltered from the wind, or (2) surrounded by close vegetation (<5 m away and of 5 m in height), or (3) in full shade, or (4) in the rain.

When a tortoise was inactive, core temperature remained within the set thermal thresholds (i.e., above LTT and below UTT) 100% of the day with a median core temperature of 28.3°C (Table 10.1). Activity had a limited impact on median temperature (an increase of 0.4°C); however, activity did reduce time within the set thermal thresholds to 82% of total time. Maximum predicted core temperature was 33.4°C, an increase of 1.5°C from the inactive scenario. Paradoxically, despite metabolic heat production, minimum core temperature (T_b) with activity was 0.6°C lower than the inactive scenario. The paradox is explained because in the case of active tortoises the plastron is assumed not to be in contact with the ground, which eliminates heat transfer through conduction. Shelter from wind had a moderate effect on core temperature, increasing the median by 2°C from an inactive tortoise model, and resulting in 80% of total time within core temperature thresholds. The remaining scenarios all had relatively large impacts on core temperature (Table 10.2). Proximity to vegetation (5 m) decreased median core temperature by 5°C from 28.3°C to 23.5°C, with 90% of total time below minimum T_b, and just 10% within the tolerable temperature range. Full shade resulted in the most extreme departure from the base case, with maximum, median, and minimum T_b being 12.6°C, 9.4°C, and 6.6°C below base case predictions, respectively. Finally, presence of rain led to 100% of the time below minimum T_b, with minimum and maximum

TABLE 10.1 The effect of individual behavioral thermoregulatory options on the core temperature of Galapagos tortoises.

Thermoregulatory state	% >UTT	% in Thresholds	% <LTT	Maximum T_b	Median T_b	Minimum T_b
Inactive	0	100	0	31.9	28.3	25.3
Active	10	82	8	33.4	28.7	24.7
Shelter from wind	20	80	0	34.1	30.3	27
Close vegetation	0	10	90	25.1	23.3	21.8
Shade	0	0	100	19.3	16	18.7
Rain	0	0	100	22.6	21.4	20.5

Base case scenario presented here is for a 200-kg tortoise at an elevation of 400 m in September. All temperatures are in °C. The gray-shaded cells indicate values outside of the set thermal tolerance range. *LTT*, Lower thermal threshold; *UTT*, upper thermal threshold.

TABLE 10.2 Predicted core body temperature (T_b) values for Galapagos tortoises of varying body size across a range of elevations on Santa Cruz Island, Galapagos during the cool season (September).

Body mass (kg)	Elevation (m)	% >UTT	% in Thresholds	% <LTT	Maximum T_b	Median T_b	Minimum T_b
2	10	38	16	46	49	27	17
50		55	45	0	44	34	26
200		73	27	0	42	36	31
2	100	33	15	53	44	24	17
50		41	47	12	40	31	24
200		51	49	0	39	33	28
2	200	21	22	58	36	23	19
50		19	62	19	35	28	24
200		20	80	0	34	30	27
2	300	15	24	61	35	22	18
50		10	60	30	33	27	23
200		0	100	0	33	29	26
2	400	8	29	63	33	21	17
50		0	62	38	32	26	22
200		0	100	0	32	28	25
2	500	0	30	70	29	20	18
50		0	46	54	29	25	21
200		0	74	26	29	26	24

The gray-shaded cells indicate values outside of core temperature thresholds. *LTT*, Lower thermal threshold; *UTT*, upper thermal threshold.

core temperatures of 20.5°C and 22.6°C, respectively (Table 10.1; Fig. 10.8).

Tortoise distribution over an elevation gradient

On larger and higher islands and volcanoes, Galapagos tortoises undergo annual migrations along an elevation gradient, driven by the distribution of forage quality and quantity (Blake *et al.* 2013; Yackulic *et al.* 2017; Chapter 13: Movement Ecology). On Santa Cruz Island, where migrations are best studied, tortoises move between c. 0 and 400 m in elevation. Tortoises are in the coolest, highest part of their range during the coolest months, and the hottest, lowest part of their range (the lowlands) during the hottest months; thus migratory tortoises crisscross temperature extremes during the year (Fig. 10.3). Field observations and data from GPS-tagged tortoises indicate that migration is size-biased: large individuals migrate higher up the elevation gradient than do smaller tortoises. Why larger tortoises migrate to higher, cooler zones has been described in some detail (Bastille-Rousseau *et al.* 2019; Blake *et al.* 2013; Yackulic *et al.* 2017; Chapter 13: Movement Ecology) but reasons why smaller tortoises stay at lower elevations remain unclear, although it is perhaps due to the lower absolute food requirements of smaller tortoises compared to larger ones. Rainfall and vegetation productivity increase with elevation (Blake *et al.* 2013; Cayot 1987); therefore to meet their forage intake requirements, large tortoises may need to travel to higher elevations.

An alternative explanation for larger tortoises migrating to higher elevations, which has received little attention to date, may lie in thermal ecology as hinted at in Fig. 10.2. As elevation increases, ambient temperature declines, while wind speed, humidity, and rainfall increase. Plants respond to these same drivers, such that higher elevations have more lush plant growth, and, by extension, more and higher quality tortoise forage. Given this, if tortoises are positioning themselves vertically along the slopes of the islands to maximize food availability while remaining within core temperature thresholds above the LTT, larger body size might buffer

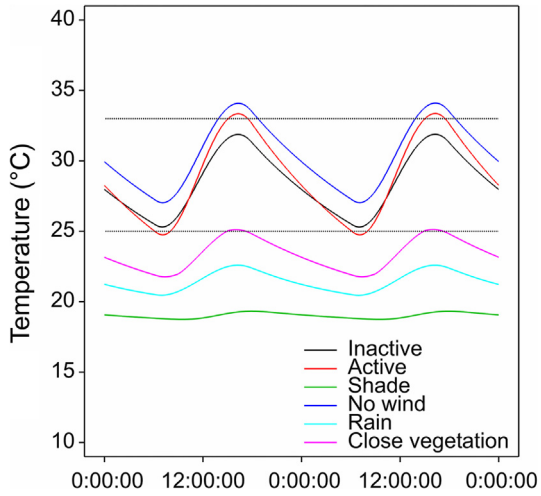

FIGURE 10.8 How Galapagos tortoise thermoregulatory behavior affects core temperature of a 200-kg tortoise in the coolest month (September) at the coolest elevation (400 m) on Santa Cruz Island. The horizontal dashed lines represent estimated thermal thresholds for core temperature (LTT and UTT). Highest core temperatures, which just exceed upper thermal tolerance, are achieved by an inactive tortoise in the open and sheltered from the wind. An active tortoise in the open exceeds both upper and lower thermal tolerance thresholds, while an inactive tortoise remains within thermal tolerance at all times. Proximity to vegetation (5 m away from the tortoise and 5 m in height), rain, and particularly shade maintain core temperature below the lower tolerance threshold. *LTT*, Lower thermal threshold; *UTT*, upper thermal threshold.

tortoises against cooler conditions and enable larger bodied tortoises to move to higher elevations where forage is more available.

The hypothesis that larger body size buffers tortoises sufficiently against cooler temperatures at higher elevations was investigated by first modeling core temperature profiles of tortoises from 2 to 200 kg over an elevation gradient in 100-m increments (Table 10.2; Fig. 10.9). Second, from these predictions the maximum elevation a tortoise of a given body mass could attain while remaining within its thermal tolerance range was calculated (Fig. 10.8). These predictions were then tested against tortoise distribution data collected during field surveys every month between 2009 and 2017. Monthly surveys involved walking a consistent "path of least resistance" from 50 to 400 m elevation, recording the size, sex, and location of each tortoise encountered within 20 m of the survey trail (Blake *et al.* 2013). Using survey data collected each September, the size threshold associated with the smallest 10% of tortoises encountered within ±5 m of each 50 m elevation increment (e.g., 45−55 m, 95−105 m) was estimated.

Relationships between tortoise body mass versus elevation for both the field data and the model predictions (Fig. 10.9) indicate that, at 10 m elevation, the predicted core temperature of a 2-kg tortoise varied widely between

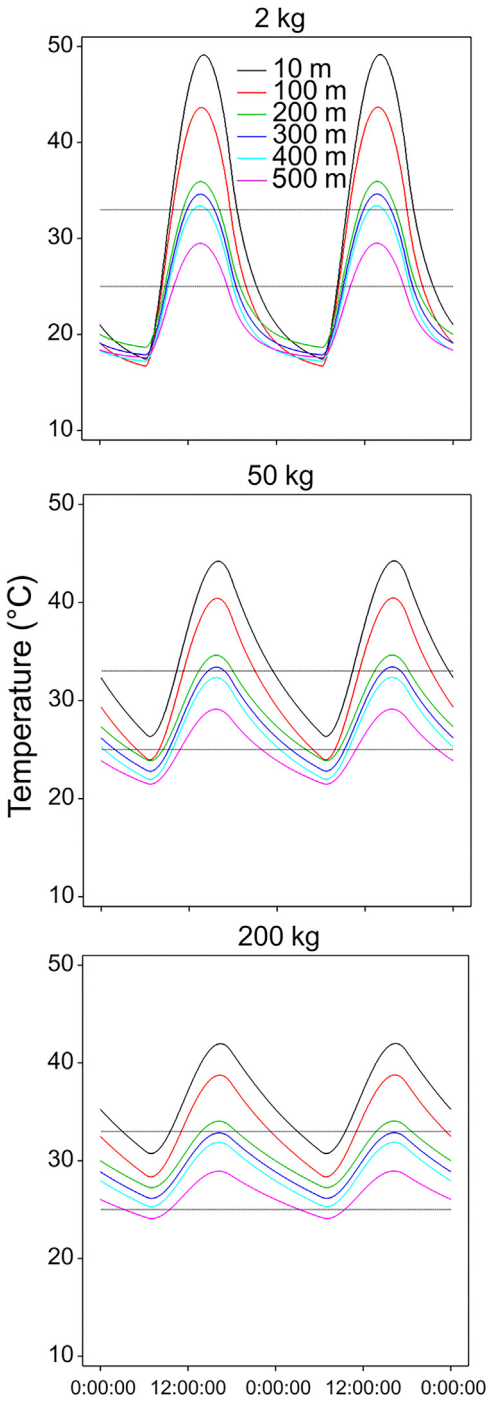

FIGURE 10.9 Variation in core temperature (T_b) with elevation for tortoises of 2-, 50-, and 200-kg body mass on Santa Cruz Island in September, the coolest month, under general conditions—tortoises inactive, in the open, far from vegetation, and exposed to wind and no rainfall. At all elevations, small tortoises fail to maintain core temperature above the lower thermal threshold, and at all elevations below 500 m, the upper thermal threshold is exceeded. Maximum and minimum core temperatures are less extreme as tortoise body size increases due to thermal inertia; however, the only situation under which a tortoise remains within thermal tolerance is a 200-kg individual at 300 and 400 m.

TABLE 10.3 Effects of thermoregulatory strategies on core temperature profiles of Galapagos tortoises of varying body size under hottest situations (at 10 m elevation in March on Santa Cruz Island).

Thermoregulatory state	Body mass (kg)	% >UTT	% in Thresholds	% <LTT	Maximum T_b	Median T_b	Minimum T_b
Active	2	43	10	46	65.6	27.6	13.0
Passive		43	15	42	54.5	28.6	16.1
Active and shade between 7 a.m. and 5 p.m.		0	28	72	29.4	19.5	13.6
Active and shade between 7 a.m. and 5 p.m., close vegetation		0	35	65	29.7	22.9	20.0
Active and hourly shade between 7 a.m. and 5 p.m.		28	21	51	49.0	24.7	19.8
Active, shade, sun between 3 and 5 p.m.		0	61	39	31.6	25.6	24.3
Active	200	76	24	0	49.0	38.7	29.9
Passive		76	24	0	43.9	36.9	30.8
Passive and wind at 200%		66	34	0	42.0	35.3	29.5
Passive and close vegetation		81	19	0	42.1	36.2	31.8
Passive and shade		0	100	0	27.9	27.3	26.7
Passive and rain		0	100	0	32.0	29.9	28.4
Passive, shade, and rain		0	59	41	26.2	25.2	24.5
Active between 7 a.m. and 5 p.m., shade, and rain		0	63	37	26.4	25.3	24.5
Active between 7 a.m. and 5 p.m., shade		0	100	0	28.3	27.5	26.9
Active and shade between 7 a.m. and 5 p.m.		0	26	74	25.7	24.2	23.1

The gray-shaded cells indicate values outside core temperature thresholds. Large tortoises can maintain temperatures within thresholds if they can find shade. Small tortoises can also avoid overheating with shade but are unable to avoid falling below LTT at night. *LTT*, Lower thermal threshold; *UTT*, upper thermal threshold.

17°C and 49°C with a median of 27°C, and 38% and 46% of a given day above and below UTT and LTT, respectively (Table 10.3; Fig. 10.5). By contrast, core temperature of a 200-kg tortoise never fell below the LTT, but for 73% of the time it was above the UTT, attaining a maximum T_b of 42°C (Fig. 10.9). At 10 m elevation, all size classes of tortoises exceeded UTT for sustained periods. Core temperatures of 200-kg tortoises were predicted to exceed UTT at elevations at or below 300 m, while 2- and 50-kg tortoises required an elevation of 400 m or above to avoid exceeding UTT. The only condition under which core temperature was maintained within thermal limits was a 200-kg tortoise at 300−400 m; at 500 m, 200-kg tortoises sustained core temperatures below LTT for 26% of the time. Large tortoises were able to withstand night-time cooling more effectively than smaller individuals: a 2-kg tortoise failed to maintain core temperatures above LTT at any elevation, whereas a 200-kg tortoise only dipped below LTT at 500 m (Table 10.3; Fig. 10.9), which is just beyond the upper limit of the cool season migration on Santa Cruz Island (Blake *et al.* 2013).

If shade is available, tortoises can avoid overheating during hot ambient conditions by behaviorally thermoregulating, that is, moving to a shade patch to cool down. However, tortoises have fewer behavioral options open to them to avoid excessive cooling when local conditions are cold. In the absence of hot volcanic soils, which are present on some islands, tortoises are limited to keeping out of wind and rain and finding shelter at night. Minimum T_b of tortoises in September including full shade from 5 p.m. to 7 a.m. was examined over the range of body masses and elevations considered in the model (2−200 kg and 10−500 m), respectively. Using these

conditions, the predicted maximum elevation at which tortoises of different masses could maintain core temperature above LTT was calculated. Field data showed remarkable congruence with the maximum elevation limits predicted by the model (Fig. 10.10). Two conclusions are noteworthy. First, predictions match the field data, which gives confidence in the biological relevance and validity of the model (Figs. 10.4 and 10.5). Second, the hypothesis concerning the role of thermoregulation as a primary determinant of elevation limits for tortoises during seasonal migrations is supported, that is, the upper elevation limits of tortoise distribution is likely determined by the interaction among minimum environmental temperatures, behavioral thermoregulation, and tortoise body mass.

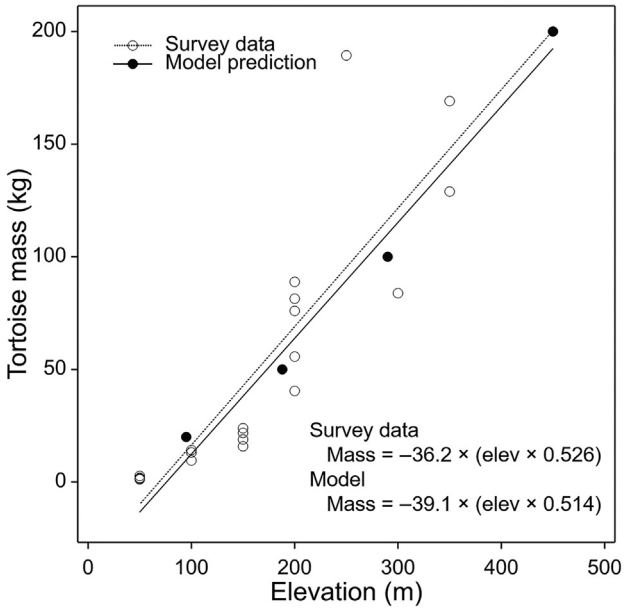

FIGURE 10.10 The relationship between the predicted elevation at which tortoises of different body mass maintain minimum core temperature at or above the lower thermal threshold in September and the threshold size of the smallest 10% of tortoises observed in the field at each elevation on surveys in September.

Thermoregulation during the hot season

Having established the importance of minimum temperatures in determining the elevational limits to tortoise distribution during the upland phase of the migration, it is also important to consider how tortoises shed heat while in the lowlands (the hottest location) in March (the hottest month). Tortoises of all size classes occur in the lowlands during March, typically the only time of the year when rainfall and vegetation productivity there are high. The propensity for overheating even during the cool season when shade is not present (Fig. 10.8) provokes two important questions: first, using plausible field conditions, can tortoises remain within core temperature thresholds via thermoregulation? And, if so, which thermoregulatory strategies can tortoises employ across their full range of body size to accomplish this?

Via a combination of activity and shade through the day, a 200-kg tortoise can evidently maintain its core temperature within upper and lower thresholds with shade being by far the most important factor in reducing daytime core temperature (Table 10.4; Fig. 10.11). The general scenario predicted 76% of total time above UTT,

TABLE 10.4 Predictions of current ambient temperature and altostratus cloud cover and future climate scenarios (2°C ambient temperature increase and cirrostratus cloud cover) on core temperature profiles of Galapagos tortoises of varying size during hot conditions at 10 m elevation in March on Santa Cruz Island.

Thermoregulatory state (kg)	% >UTT	% in Thresholds	% <LTT	Maximum T_b	Median T_b	Minimum T_b
Current climate scenario						
2	26	22	51	45.5	24.6	21.0
50	27	73	0	36.1	29.5	25.4
200	26	74	0	34.3	30.9	27.9
Climate change scenario						
2	30	32	37	47.5	26.6	23.1
50	38	62	0	37.9	31.3	27.3
200	43	57	0	35.9	32.5	29.6

The gray-shaded cells indicate values outside core temperature thresholds. Under the climate change scenario, large tortoises spend over 10% less time within thermal thresholds and more time above UTT, while small tortoises increase their time within thermal thresholds by 10%. Under climate change the small tortoise is 14% less thermally stressed by low temperature and only 4% more stressed by excessive temperature than the large tortoise. *LTT*, Lower thermal threshold; *UTT*, upper thermal threshold.

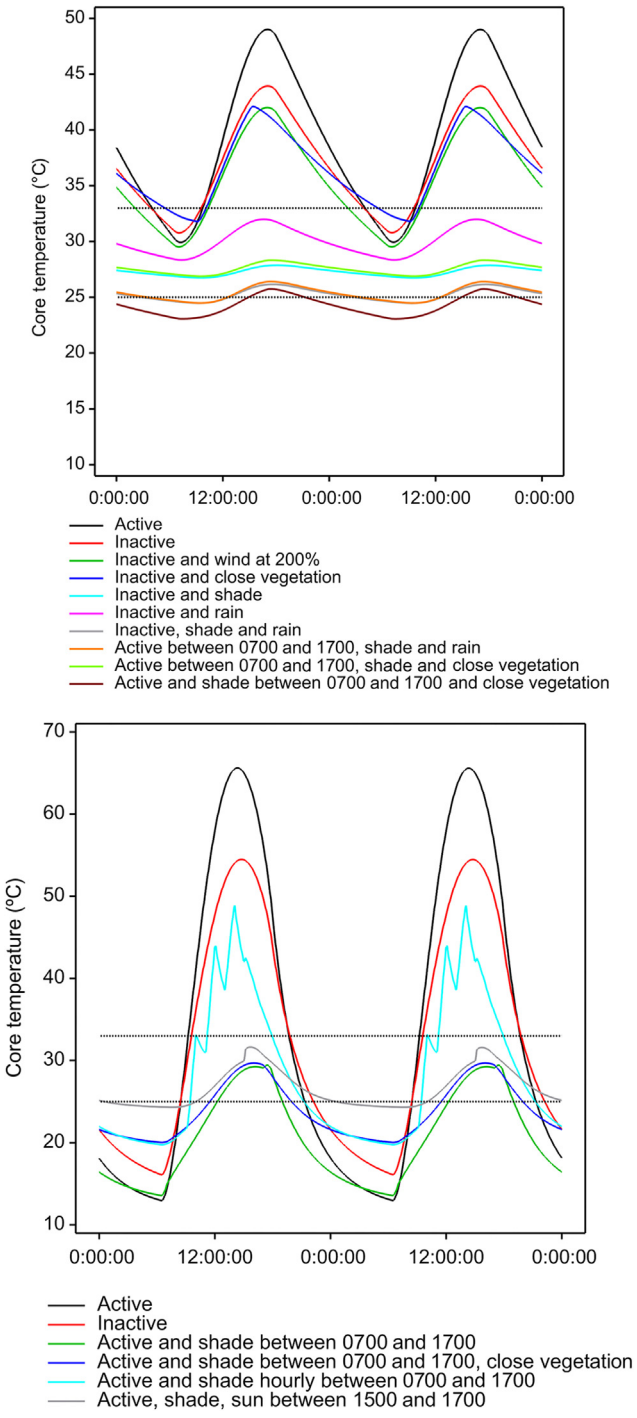

FIGURE 10.11 Effects of behavioral thermoregulation on core temperature for a 200-kg tortoise (top) and a 2-kg tortoise (bottom), at the hottest location (10 m elevation) and the hottest period (March). For both large and small tortoises, avoiding overheating is critical, and finding shade is the most effective way to maintain temperatures below the upper thermal threshold, though inactivity, wind, and rain are helpful for large tortoises. Small tortoises must use shade to cool but also need cover to avoid losing excessive heat at night. Even at the hottest location in the hottest month, core temperatures of small tortoises fall below the lower thermal threshold.

FIGURE 10.12 Hatchling Galapagos tortoises spend a considerable amount of time in thermal refuges under rocks in the shade. This helps hatchlings to keep cool during the day and retain heat at night. *Photo: Stephen Blake.*

28% of total time within core temperature thresholds, and 0% below LTT. Activity increased daily median T_b by c. 5°C from the passive state, but only increased daily minimum T_b by c. 1°C. Exposure to strong wind (twice that of mean March wind speed) increased time within core temperature thresholds by 6% compared to the general case. Shade and rain combined with an inactive state meant the 200-kg tortoise was within thermal thresholds 100% of the time, as might happen in terms of continuous inactivity and exposure to continuous rain that tortoises must face during El Niño periods. If a 200-kg tortoise was active between 7 a.m. and 5 p.m., in permanent shade and close to vegetation, it would likely remain within a tolerable core temperature range. A tortoise under the same conditions, but in the open at night (5 p.m. to 7 a.m.), was predicted to be within core temperature thresholds just 26% of the time, and below LTT 74% of total time. Thus a large tortoise can shed enough heat even under the hottest conditions if it can find shade to avoid direct sun exposure during the day and, if necessary to shed excess heat at night, move into the open to emit radiant heat to the sky.

In contrast to a large tortoise, a 2-kg tortoise at 10 m elevation in March is evidently unable to maintain core temperature >LTT for more than 61% of total time. By remaining in the shade and close to vegetation during the day, a small tortoise can avoid overheating but is unable to retain enough heat at night under any thermoregulation scenarios to avoid T_b falling below LTT (Table 10.3). Intermittent short duration bursts of exposure to sun through the day followed by periods in the shade (Table 10.3; Fig. 10.11) will allow a 2-kg tortoise to prolong its total time within thermal tolerance thresholds; however, it will always lose heat rapidly as sunlight fades. Thus, even under the hottest conditions, if a small tortoise

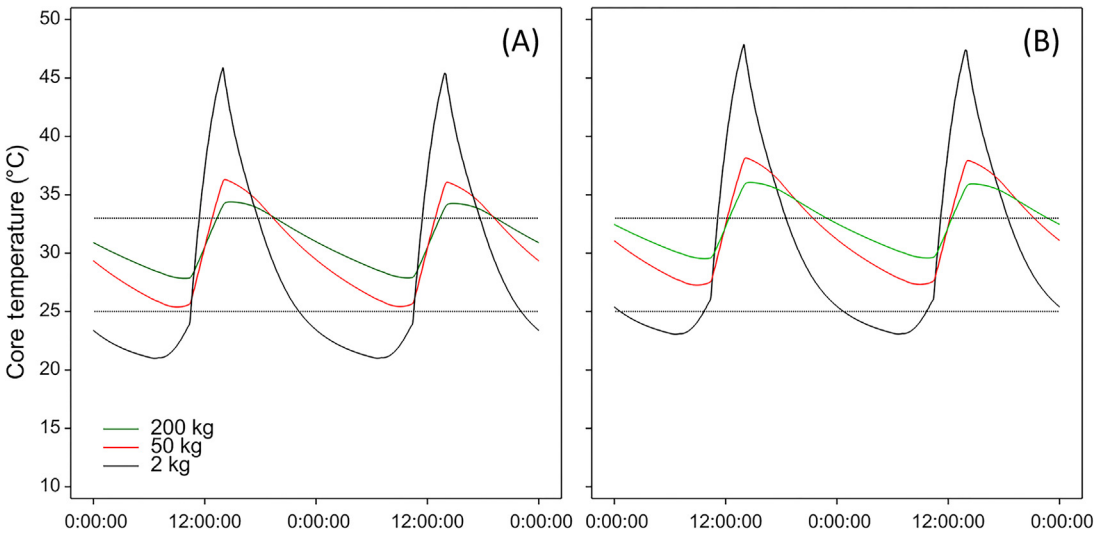

FIGURE 10.13 Model predictions on the core temperature profiles for tortoises weighing 2, 50, and 200 kg (A) at 10 m elevation, active between 7 a.m. and 5 p.m. in shade and with proximity to vegetation, in March, (B) under the same conditions except an ambient temperature increase of 2°C and cloud cover of cirrostratus to simulate a plausible climate change scenario. If shade can be found under the climate change scenario, tortoises of all size classes can avoid overheating both currently and with climate change. Climate change may help the smallest tortoises avoid excessive cooling at night.

can find shade, it will be thermally stressed not by high temperatures, but rather by low temperatures it cannot avoid during the night (Fig. 10.12).

Climate change impacts on Galapagos tortoises

Predicting the impact of anthropogenic factors on future climactic conditions is problematic, even at global scales, due to the complexity of climate systems and their poorly understood interactions with greenhouse gas fluxes, deforestation, and other land-use and human-induced environmental changes (Schindler and Hilborn 2015; Chapter 16: Climate Change). Predictions become progressively more fraught at smaller spatial scales. Modeling future climate scenarios on Galapagos is particularly difficult because of its location in the climactically variable eastern Pacific, with weather patterns and land temperatures that are largely dependent on sea surface temperatures and prevailing oceanic currents (Colinvaux 1984:55–69; Liu *et al.* 2013; Sachs and Ladd 2010; Trueman and d'Ozouville 2010). Moreover, applying current climate change scenarios to the modeling approach to predict impacts on tortoise heat balance would require knowledge of the scale of change to all the input variables, or at least the important ones (Table 10.A1). Ambient temperature, cloud cover, rainfall, vegetation characteristics, and other factors will all interact to determine microclimate variability and thermoregulatory options available to tortoises in the future.

Despite these uncertainties and unknowns, the heat-balance model (Fig. 10.4) provides a framework in which to generate and test hypotheses on how future environmental change might influence tortoise heat balance. For example, many climate scientists agree (Bathiany *et al.* 2018; Hoegh-Guldberg *et al.* 2019) that a 2°C rise in global mean temperature is likely before the end of this century—well within the lifetime of many Galapagos tortoises alive today. It is also likely that cloud cover will decline markedly (Zelinka *et al.* 2020). What could this mean for tortoises during the hottest month at the hottest elevation?

Under a 2°C increase in ambient temperature and a shift from altostratus to cirrostratus clouds (all other conditions remaining equal), implications diverge for tortoises of different body sizes: a 2-kg tortoise is expected to spend more time within its thermal tolerance range, while large tortoises are predicted to spend less (Table 10.4; Fig. 10.13). A 2-kg tortoise that is active from 7 to 10 a.m. and 3 to 5 p.m. in the open but close to 5-m-tall vegetation will remain within thermal thresholds for 32% of the time compared to 22% of the time under current conditions, and only 4% more time above UTT. In contrast, a 200-kg tortoise will, under this climate change scenario, spend 17% less time within thermal thresholds and 17% more time above UTT, never falling below LTT in either scenario. A 50-kg tortoise is also penalized but to a lesser extent.

This climate scenario is therefore likely to be generally beneficial to hatchling and smaller tortoises by maintaining their core temperatures above LTT for longer periods, if they can find shade during the day to reduce overheating. Indeed, even under current conditions, shade is critical for tortoises of any size—to prevent overheating during the day and excessive cooling for smaller tortoises at night.

TABLE 10.5 Due to the impact of shade from the canopy of Cuban cedars (*Cedrela odorata*), an invasive tree species, a 200-kg tortoise on Santa Cruz Island would fail to maintain its core temperature above the lower thermal threshold at various elevations during the cool season range.

Elevation	Shade/open	% >UTT	% in Thresholds	% <LTT	Maximum T_b	Median T_b	Minimum T_b
400	Open	0	100	0	31.9	28.3	25.3
400	Shade	0	0	100	19.3	19.0	18.7
300	Open	0	100	0	32.9	29.2	26.2
300	Shade	0	0	100	20.2	19.8	19.6
200	Open	20	80	0	34.1	30.4	27.3
200	Shade	0	0	100	21.0	20.7	20.4
100	Open	51	49	0	38.8	33.1	28.4
100	Shade	0	0	100	21.8	21.4	21.1

The gray-shaded cells indicate values outside core temperature thresholds. *LTT*, Lower thermal threshold; *UTT*, upper thermal threshold.

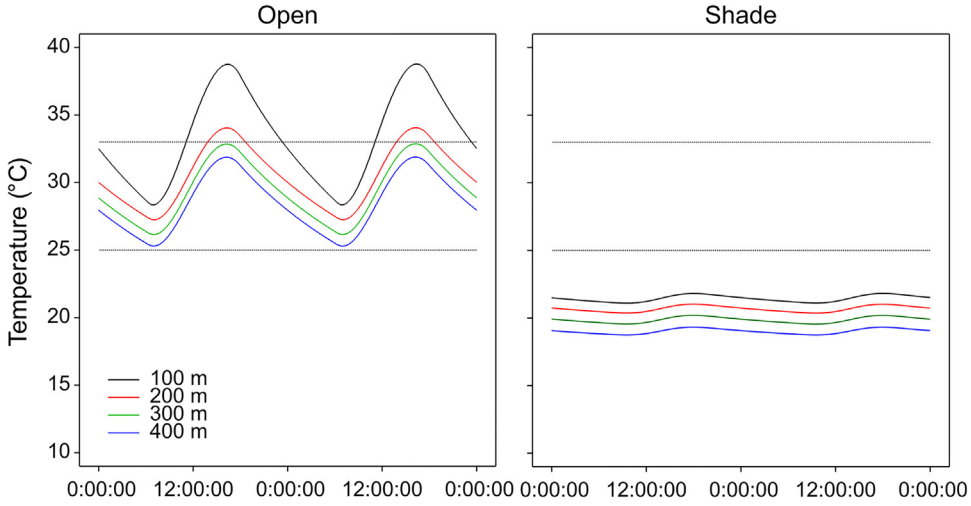

FIGURE 10.14 The expansion of Cuban cedar forests could pose a serious risk to the continued long-distance migration of tortoises, due to the impacts of shade on thermoregulation during the cool season. A 200-kg Santa Cruz tortoise in the open over a range of elevations in September (the coolest month during the upland phase of the migration) is predicted to overheat at 100 and 200 m elevation but remains within thermal tolerance at 300 and 400 m, the normal elevation range of the upland migration (Open). Under the simulated effect of a Cuban cedar forest canopy (Shade), the 200-kg tortoise is well below the lower thermal threshold at all times and all elevations.

Shade and the spread of invasive Cuban cedar

Cuban cedar (*Cedrela odorata*, Meliaceae) is a highly invasive tree species originally brought to Galapagos as a source of timber. Since its introduction into farmland, Cuban cedar has spread extensively across large areas of the humid and upper transition zone of inhabited islands, including enormous expanses inside the national park, particularly on the southwestern slopes of Santa Cruz. The potential for dense stands of Cuban cedar to block tortoise migration routes is discussed in Chapter 13, Movement Ecology, in the context of the physical difficulty it poses to tortoise mobility. However, Cuban cedar may also have implications for tortoise thermoregulation. The dense canopy produced by these trees blocks solar radiation to the forest floor resulting in extremely low light levels. Given that solar radiation is the single most important source of heat for tortoises, Cuban cedars could reduce the ability of tortoises to maintain internal temperature particularly because tortoises are most likely to encounter Cuban cedar forests in the uplands at the coolest time of the year (Table 10.5; Fig. 10.14). Clearly, the assumption of complete shade in a Cuban cedar forest is an unlikely exaggeration due to the presence of gaps in the canopy, but the central point remains that tortoises across their range would be severely limited in their ability to thermoregulate under a scenario of increasing proliferation of this invasive species.

Conclusion

The maintenance of core body temperature within physiologically tolerable limits is among the most fundamental biological requirements of all complex animals. Ectotherms, such as giant tortoises, face unique challenges compared with endotherms because their core temperature is mostly dependent on heat balances between the animal's core tissue mass and the environment and not, as is the case for endotherms, through the production of metabolic heat and the associated physiological homeostatic mechanisms that maintain stable internal temperature conditions. The evolutionary ecology of how ectotherms achieve and maintain suitable internal thermal conditions remains a major field of research. Moreover, in a rapidly changing global environment under unprecedented anthropogenic influence, there is a pressing need to understand how ectothermic organisms may fare as climate change impacts become manifest.

Understanding the capability of large, long-lived ectothermic species to withstand climate change and other forms of environmental change (e.g., habitat degradation, fragmentation, and range reduction) depends in part on quantifying their abilities to thermoregulate under a variety of current and novel conditions. Evolutionary adaptation over decadal time scales is not an option for species such as Galapagos tortoises, which may live well in excess of 150 years, making plasticity in behavioral thermoregulation of central importance in thermal homeostasis.

However, behavioral plasticity in thermoregulation necessary to keep core temperature within thermal thresholds will only be possible if tortoises have such plasticity, and the matrix of habitats within which such behaviors occur is available. If hot wet seasonal ambient temperature on Galapagos increases by 2°C in the next 50 years, and cloud cover declines by 50%, large and small tortoises during the day must have shade from vegetation available to avoid overheating, and small tortoises will require it at night to reduce heat loss to the sky. If migration corridors are no longer available (Chapter 13: Movement Ecology) to allow tortoises to access cool temperatures and back up food resources, can they avoid excessive core temperatures in the lowlands? Which combination of vegetation categories should land-owners in agricultural areas favor to provide suitable thermal conditions for giant tortoises? These issues require answers that are currently unavailable. Thermal biology matters. Giant tortoises that make poor decisions (remaining foraging in the sun) can die within an hour and in sight of shade, while longer term fitness consequences can be manifest from suboptimal thermal environments.

Deficits in the theoretical and empirical understanding of thermoregulation of Galapagos tortoises, tied to science-based conservation action, motivated development of the dynamic and predictive heat-balance model presented in this chapter. Understanding the thermal biology of Galapagos giant tortoises, iconic ectotherms, is in its infancy, at a time when the Galapagos Islands are facing rapid environmental change. The predictive tool presented here provides a quantitative framework to investigate the impacts of the interaction between environment, body size, and behavior on the thermal biology of Galapagos tortoises, the largest (with juveniles among the smallest) terrestrial ectotherms left on Earth.

Appendix 10.1 Details of Galapagos giant tortoise thermoregulation model (as developed by Nigel J. Blake)

Model basis

Model predictions

This model predicts the internal (core) temperature, the external carapace, and the plastron temperatures for Galapagos tortoises by solving a series of seven heat balances:

1. the tortoise's carapace,
2. the section of the tortoise's plastron in direct contact with the ground,
3. the section of the tortoise's plastron not in direct contact with the ground,
4. the tortoise's internal tissues,
5. open ground adjacent to the tortoise,
6. the ground under and in contact with the tortoise's plastron, and
7. the ground under but not in contact with the tortoise's plastron.

Tortoise geometry

The model considers a tortoise as a hemisphere, which is a good approximation to the shape of domed tortoises. No account is currently taken for the limbs and tail nor head and neck.

Variables

The model to calculate the core temperature of tortoises is used in two ways:

- Using field weather data, its predictions were compared with measured body temperatures over 24-hour periods.
- Having been validated, it can then be used to determine how the body temperature of tortoises of different sizes can be predicted over a wide range of weather conditions.

Weather condition data required as inputs:

- radiative heat from the sun which chiefly depends on the location of the tortoise, time of the year, and clarity of the sky;
- wind speed;
- air temperature; and
- rainfall rate.

Tortoise data required as inputs:

- location of tortoise whether in shade or near surrounding vegetation,
- activity of the tortoise,
- size of the tortoise,
- physical properties of the tortoise, and
- physical properties of the soil beneath the tortoise.

Weather conditions

Solar radiation

The solar radiation arrives from the sun as a direct beam plus scattered radiation or as radiation via a cloudy sky. The value of these terms is calculated using the methodology recommended by The American Society of Heating, Refrigerating and Air-Conditioning Engineers (ASHRAE) (Wang 2001).

Direct and scattered radiation

Direct solar radiation at the edge of the atmosphere

At the edge of the atmosphere radiation is given by:

$$I_{DN} = \frac{A \cdot C_n}{\exp(B/\sin(hs))} \tag{10.A1}$$

where I_{DN} is the intensity (flux) of solar radiation at the outer edge of the atmosphere onto a plane normal to the beam (W/m^2); C_n the clearness number of the sky (dimensionless). Figure 3.8 in Wang (2001) shows values for this parameter in the United States. A value of 1.0 is adopted for the Galapagos Islands. A is the apparent solar radiation (W/m^2) when air mass = 0; B the atmospheric extinction coefficient (dimensionless); and hs the elevation of the sun from horizontal (degrees). [Note: The zenith angle of the sun is $(90^\circ - hs)$.]

Values of A and B are given in Table 3.6 in Wang (2001), they vary according to a yearly cycle and can be correlated against n (day of the year from the 1st January) using a cosine function.

$$A = 3.15459\,(24.54\cos[0.01721\,(n - 1.4)] + 368.4) \tag{10.A2}$$

$$B = 0.03475\cos[0.01721(n - 189.8)] + 0.1717 \tag{10.A3}$$

The clear-sky diffuse solar radiation onto a surface at an angle Σ to the horizontal plane is obtained from:

$$I_d = \frac{CI_{DN}F_{ss}}{C_n^2} \tag{10.A4}$$

$$C = 0.04116\cos[0.01721(n - 187.4)] + 0.09043 \tag{10.A5}$$

$$F_{ss} = \frac{(1 + \cos\Sigma)}{2} \tag{10.A6}$$

where I_d is the intensity (flux) of clear-sky diffuse solar radiation at the earth's surface (W/m^2); C the diffuse radiation factor (dimensionless). Given in Table 3.6 in Wang (2001) and again correlated using a cosine function; F_{ss} is the shape factor between surface in question and the sky (dimensionless). For a horizontal surface the value is 1.0, a vertical surface 0.5, and a hemispherical tortoise the value can be shown to be 0.75. Σ is the angle of tilted surface to the horizontal plane (degrees or radians to suit).

The total radiation onto a horizontal surface is determined by summing the direct radiation (Eq. 10.A1) resolved normal to the horizontal and the diffuse radiation (Eq. 10.A4).

$$I_{GH} = I_{DH} + I_{dh} = I_{DN}\left(\sin(hs) + \frac{C}{C_n}\right) \tag{10.A7}$$

where I_{GH} is the total solar radiation onto a horizontal plane (W/m^2); I_{DH} the direct solar radiation onto a horizontal plane (W/m^2); I_{dh} the diffuse solar radiation onto a horizontal plane (W/m^2); and I_{DN} the direct solar radiation onto a plane normal to the radiation (W/m^2).

Radiation on a cloudy day

The reduction in solar radiation due to cloud cover (I_G^*) is treated as follows (superscript * is used for terms incorporating the effect of cloud cover). For cloudy skies, I_G^* is modeled as:

$$I_{GH}^* = \left(1 + \frac{C_{cc}Q}{P} + \frac{C_{cc}^2R}{P}\right)I_{GH} \tag{10.A8}$$

$$C_{cc} = C_T - 0.5\sum_{j=1}^{4} C_{cir,\,j} \tag{10.A9}$$

where C_{cc} is the indicates cloud cover on a scale of 0−10 (0 is a clear sky); P, Q, and R are the seasonally dependent variables; C_T is the total cloud amount (0−10); $C_{cir,\,j}$ are the clouds covered by cirriforms (including cirrostratus, cirrocumulus, and cirrus) in $j = 1-4$ layers. These four parameters are likely to be very difficult to obtain. So C_{cc} is taken as C_T but reduced by an estimated amount if the primary cloud type is cirriform.

The values of P, Q, and R for the four seasons of the year are given on page 3.28 (Wang 2001). This method of calculating direct and diffuse solar radiation is for US weather

stations; therefore there is some doubt that the seasonal values for P, Q, and R are appropriate for the Galapagos, where the seasons are not the same. Their influence over the final solar fluxes is, however, relatively minor compared with other larger uncertainties such as cloud cover.

The direct and diffuse solar fluxes from a cloudy sky onto a horizontal plane are then given by:

$$I^*_{DH} = \frac{I^*_{GH}\sin(hs)\cdot\left(1-\left(C_{cc}/10\right)\right)}{\sin(hs)+C/C_n^2} \tag{10.A10}$$

$$I^*_{dH} = I^*_{GH} - I^*_{DH} \tag{10.A11}$$

Finally, the two key radiation fluxes from the sun impacting the tortoise can be determined as follows:

- I^*_{DN}—the direct flux under a cloudy sky in a plane normal to the sun's rays and
- $I^*_{d\Sigma}$—the diffuse flux under a cloudy sky onto a surface at an angle of Σ to the horizontal, for which F_{ss} has the value of 0.75 (appropriate for a hemispherical tortoise).

$$I^*_{DN} = \frac{I^*_{DH}}{\sin(hs)} \tag{10.A12}$$

$$I^*_{d\Sigma} = I^*_{dH}F_{ss} \tag{10.A13}$$

Elevation of sun as a function of date and time

The final parameter that is required for determining the radiation intensity at a site central to the Galapagos Archipelago—Puerto Ayora—at a longitude of −90.32 degrees is the sun's elevation (hs). The mathematical relationships for the sun elevation as a function of location, date, and time is given by an online article (https://en.wikipedia.org/wiki/Position_of_the_Sun).

Daily ambient temperature

Ambient temperature throughout the day is modeled as a sinusoidal form between the daily maximum and minimum temperatures (between user-defined start and end times) and constant at the daily minimum temperature at other times. Field data from Santa Cruz Island in Galapagos suggest there are several types of daily temperature trends during different seasons (Blake, unpubl. data), but a general one is for the ambient temperature to start rising from its minimum value at 0700 hours and to return to this value at about 2100 hours.

The expression for ambient temperature used between start and end times for the sinusoidal profile is:

$$T_a = \frac{(T_{amax}-T_{amin})}{2}\cdot\cos\left[\left(\frac{2\,\pi}{(h_{end}-h_{start})}\right)\cdot\left(h-\left(\frac{h_{start}+h_{end}}{2}\right)\right)\right]+\left(\frac{T_{amax}+T_{amin}}{2}\right)$$

where h is the hour of the day as a decimal (e.g., 0830 = 8.50); h_{start} the start time in day for temperature to follow sinusoidal profile (hour of the day, e.g., 0700 = 7.00); h_{end} the end time in day for temperature to follow sinusoidal profile (hour of the day, e.g., 1900 = 19.00); T_a the ambient temperature as a function of time of day (°C); T_{amax} the maximum daily ambient temperature (°C); and T_{amin} the minimum daily ambient temperature (°C).

Daily wind speed

A sinusoidal relationship is also observed for wind for Espanola Island, Galapagos (Blake, unpubl. data):

$$u = \frac{(u_{max}-u_{min})}{2}\cdot\cos\left[\left(\frac{2\,\pi}{(h_{wend}-h_{wstart})}\right)\cdot\left(h-\left(\frac{h_{wstart}+h_{wend}}{2}\right)\right)\right]+\left(\frac{u_{max}+u_{min}}{2}\right)$$

where h is the hour of the day as a decimal (e.g., 0830 = 8.50); h_{wstart} the start time in day for wind to follow sinusoidal profile (hour of the day, e.g., 0700 = 7.00); h_{wend} the end time in day for wind to follow sinusoidal profile (hour of the day, e.g., 1900 = 19.00); u the wind speed as a function of time of day (m/s); u_{max} the maximum daily wind speed (m/s); and u_{min} the minimum daily wind speed (m/s).

The start and end times for the sinusoidal profile are also approximately 0700 and 2100.

Heat flows: Carapace

Ten heat transfer mechanisms are considered for the carapace heat flows:

1. convection,
2. direct solar radiation,
3. diffuse solar radiation,
4. reflected solar radiation from ground (but not the local environment),
5. thermal radiation between ground and carapace,
6. thermal radiation between surrounding terrestrial environment and carapace,
7. thermal radiation between sky and carapace,
8. sensible heat transfer due to rain falling on carapace (where applicable),
9. latent heat by evaporation of rain film from carapace (where applicable), and
10. conduction of heat into carapace from internals (temperature gradient across carapace).

View factors for radiant heat transfer between the tortoise and the surrounding environment have been calculated using methodologies described in Bird *et al.* (1960), using standard configuration factors from Howell (2019) and where there were no solutions these were calculated using an approximation.

Convection

The heat transfer coefficient (HTC) for air flowing (convection) over the carapace is given by a standard Nusselt correlation for a sphere suspended in a free stream is given in Bird *et al.* (1960). As the tortoise is modeled as a hemisphere, the calculated HTC can be adjusted downwards by a constant factor (*hcf*), though this value is not known. This approach is used because the average velocity of air over the tortoise will be reduced by drag due to the presence of the ground compared with that over a freely suspended sphere.

The HTC and heat flux into the tortoise by air flowing over the carapace is calculated by the following equations with values for physical properties of air being taken at the average film temperature (between the carapace and ambient temperature):

$$Re = \frac{\rho_f u\, d}{\mu_f} \tag{10.A14}$$

$$Pr = \frac{C_{pa}\, \mu_f}{k_f} \tag{10.A15}$$

$$Nu_{sphere} = 2 + 0.6\, Re^{0.5} Pr^{1/3} \tag{10.A16}$$

$$h_{sphere} = \frac{Nu_{sphere}\, k_f}{d} \tag{10.A17}$$

$$h_c = hcf\,.\, h_{sphere} \tag{10.A18}$$

$$Q_c = A_{scar}\, h_c (T_a - T_1) \tag{10.A19}$$

where A_{scar} is the surface area of carapace (m^2); C_{pa} the specific heat capacity of air in film [(J/kg K) T]; d the diameter (characteristic length) of tortoise (m); h_c the HTC over carapace (W/m^2 K); *hcf* the adjustment factor on HTC for hemispherical tortoise versus sphere. Calculations in this chapter use a value of 1. k_f is the thermal conductivity of air in film (W/m K); *Nu* the Nusselt number (dimensionless); *Pr* the Prandtl number (dimensionless); Q_c the *heat rate into tortoise by forced convection over carapace (W)*; *Re* the Reynolds number (dimensionless); T_1 the carapace surface temperature (°C); T_a the ambient temperature (°C); u the wind speed (m/s); μ_f the dynamic viscosity of air in film (kg/m s); and ρ_f the density of air in film (kg/m^3).

Direct solar radiation

Calculation of the direct solar flux onto a tortoise is determined using Eq. (10.A12):

$$Q_{dir} = A_{sp}\, a_1\, I^*_{DN} \tag{10.A20}$$

where a_1 is the absorptivity of carapace to solar radiation (dimensionless); A_{sp} the projected area of hemisphere normal to direct solar radiation (m^2); I^*_{DN} the direct solar radiation flux (under clear or cloudy skies) in a plane normal to sun's rays (W/m^2); and Q_{dir} the heat rate to tortoise by direct solar radiation (W).

In the present model the tortoise is considered to be situated in open ground surrounded by a "cylinder" of vegetation (at a user-stated distance from the tortoise) which is of a user-defined height. If the sun has not risen above the top of the vegetation, then I^*_{DN} is set to zero.

Diffuse solar radiation

Calculation of the direct solar flux onto a tortoise is determined using Eq. (10.A13):

$$Q_{dif} = A_{scar}\, a_1\, I^*_{d\Sigma}\, \frac{F_{14}}{0.75} \tag{10.A21}$$

where $I^*_{d\Sigma}$ is the diffuse solar radiation flux (under clear or cloudy skies) to the carapace (W/m^2); Q_{dif} the heat rate to tortoise by diffuse solar radiation (W); and F_{14} the view factor for radiation from tortoise (surface 1) to sky (surface 4) (dimensionless).

The adjustment on flux by the factor $F_{14}/0.75$ accounts for the portion of the sky obscured by vegetation. For no vegetation present at all, the maximum value of F_{14} is 0.75; therefore the diffuse solar flux reaching the tortoise with surrounding vegetation is scaled accordingly.

Reflected solar radiation

In the case of the tortoise, it is assumed there is little reflection of solar radiation from the surrounding vegetation, but (depending on ground type) there may be nonnegligible reflected radiation from the ground. The total solar radiation flux to the ground is given by I^*_{GH} (Eq. 10.A8) and a fraction $(1 - a_2)$ is reflected isotropically. Heat rate (W) to the tortoise carapace by reflected solar radiation from the ground is therefore given by:

$$Q_{ref} = F_{12}\, A_{scar}\, a_1 (1 - a_2)\, I^*_{GH} \tag{10.A22}$$

where Q_{ref} is the heat rate to tortoise from reflected solar radiation from the ground (W); F_{ij} the view factor surface i to surface j (dimensionless). The tortoise carapace is surface 1; the ground surface 2. a_2 is the absorptivity of ground for solar radiation (=1 − ground reflectance).

Thermal radiation between ground and carapace

Radiative heat transfer between the carapace of the tortoise and the ground is governed according to the Stefan–Boltzmann equation in Bird *et al.* (1960).

$$Q_{rg} = \sigma\, A_{scar}\, F_{12} \left(e_2 T_2^4 - e_1 T_1^4\right) \tag{10.A23}$$

where e_1 is the emissivity of carapace (dimensionless); e_2 the emissivity of ground surrounding tortoise (dimensionless); Q_{rg} the heat rate to tortoise due to radiation from ground (W); T_1 the temperature of exterior of carapace (K); T_2 the temperature of ground surrounding tortoise (K); σ the Stefan–Boltzmann constant (5.67×10^{-8} W/m^2 K^4).

Thermal radiation between terrestrial environment and carapace

Radiative heat transfer between the carapace of the tortoise and the surrounding vegetative environment is governed according to the following equation:

$$Q_{rv} = \sigma A_{scar} F_{13}\left(e_3 T_3^4 - e_1 T_1^4\right) \tag{10.A24}$$

where e_3 is the emissivity of vegetation surrounding tortoise (dimensionless); Q_{rv} the heat rate to tortoise due to radiation from surrounding vegetation (W); T_3 the temperature of environment surrounding tortoise (K), which is assumed to be at ambient temperature (T_a).

Thermal radiation between sky and carapace

Radiative heat transfer between the carapace of the tortoise and the sky is governed according to the following equation:

$$Q_{rs} = \sigma A_{scar} F_{14}\left(e_4 T_4^4 - e_1 T_1^4\right) \tag{10.A25}$$

where e_4 is the emissivity of the sky (dimensionless); Q_{rs} the heat rate to tortoise due to radiation from the sky (W); and T_4 the temperature of sky (K).

Calculation of the temperature of the sky and its emissivity is not presented here.

Sensible heat transfer due to rainfall

Heat is transferred to (or more likely away from) the carapace by rain falling on its surface. If the rain film on the surface quickly reaches carapace temperature before running off at the bottom then the rate of heat transfer to the carapace is given by:

$$Q_{rains} = \rho_w F_t C_{pw} (T_{rain} - T_1) \tag{10.A26}$$

where Q_{rains} is the sensible heat rate to carapace from falling rain film (W); ρ_w the density of water (1000 kg/m^3); F_t the rainfall rate to carapace (m^3/s); C_{pw} the specific heat capacity of water (4186 J/kg K); and T_{rain} the temperature of rain (°C).

Latent heat due to evaporation of rain

The evaporation rate from the surface of the rain film on the carapace can be predicted using the Chilton–Colburn (or *j*-factor) analogy between heat, mass, and momentum transfer.

Water is evaporated due to the differential in vapor pressure (or mole fraction) between the rain film–air interface (which is assumed saturated at the film surface temperature) and bulk air. The mass transfer coefficient is given by equation 14.4–5 in Bird *et al.* (1960) and the following defining relationships:

$$Re = \frac{\rho_f u d}{\mu_f} \tag{10.A27}$$

$$Sc = \frac{\mu_f}{\rho_f D_{wf}} \tag{10.A28}$$

$$Sh_{sphere} = 2 + 0.6\, Re^{0.5} Sc^{1/3} \tag{10.A29}$$

$$k_{wm,\ sphere} = \frac{Sh_{sphere} C_f D_{wf}}{d} \tag{10.A30}$$

$$k_{wm} = hcf \cdot k_{wm,\ sphere} \tag{10.A31}$$

$$W_{wm} = k_{wm} \frac{\left(y_{w0} - y_{w,\ amb}\right)}{(1 - y_{w0})} \tag{10.A32}$$

The values for mole fraction of water at the film–air interface and bulk air are derived from the standard Antoine equation for saturated water vapor pressure in air (P_{vsat} in Pa) as a function of temperature T (in °C):

$$\dot{M} = (MW)_w \cdot W_{wm} \cdot A_{scar} \tag{10.A33}$$

If the rate of evaporation from the carapace $\dot{M}$ is greater than the rainfall rate to the carapace (the product of F_t and ρ_w), then:

$$\dot{M} = F_t \cdot \rho_w \tag{10.A34}$$

$$Q_{raine} = -L_w \cdot \dot{M} \tag{10.A35}$$

where C_f is the molar density of air (g-mole/m^3); d the diameter or characteristic length of tortoise (m); and D_{wf} the diffusion coefficient of water vapor in air at average boundary layer temperature (m^2/s). Calculated at different temperatures from a known value at a reference temperature: D_{wa} is proportional to $T^{3/2}$ (absolute temperature in K). D_{wa} (273.15K) $= 2.2 \times 10^{-5}$ m^2/s. *hcf* is the adjustment factor on mass transfer coefficient for tortoise versus sphere (dimensionless). Assumed equal to the equivalent adjustment factor for heat transfer. k_{wm} the molar mass transfer coefficient of water vapor from surface (g-mole/m^2 s); L_w the latent heat of evaporation of water (roughly constant at all temperatures considered 2.43×10^{-6} J/kg); $(MW)_w$ the molecular mass of water (0.01802 kg/g-mole); $\dot{M}$ the mass rate of water evaporating from surface of carapace (kg/s); Q_{raine} the heat rate

into the carapace by evaporation of water from its surface (W); *Re* the Reynolds number (dimensionless); *Sc* the Schmidt number (dimensionless); *Sh* the Sherwood number (dimensionless); u the wind speed (m/s); W_{wm} the mass transfer flux (molar units) of water evaporated from film (g-mole/m^2 s); $y_{w,amb}$ the mole fraction of water vapor in bulk air (dimensionless); y_{w0} the mole fraction of water vapor in air at film−air interface—saturated conditions at interface temperature (dimensionless); μ_f the dynamic viscosity of ambient air at average boundary layer temperature (kg/m s); and ρ_f the density of ambient air at average boundary layer temperature (kg/m^3) calculated from the perfect gas law.

Conduction between tortoise internal tissue mass and carapace

The heat flowing through the carapace due to the temperature driving force between carapace exterior and internal temperature must also be considered. The heat rate into the carapace is given by:

$$Q_{condc} = \frac{A_{scar} k_1 (T_i - T_1)}{x_c} \qquad (10.A36)$$

where Q_{condc} the heat rate into carapace due to conduction (W); k_1 the thermal conductivity of carapace (W/m K); T_i the internal temperature of tortoise (°C); and x_c the thickness of carapace (m).

Net heat rate into carapace

The net heat rate into the carapace (Q_{cnet}) is calculated by summing the heat rates from the previous 10 subsections. It should be noted that as a consistent sign convention has been used some of the heat rates which are likely to be negative will be calculated as negative by the earlier equations:

$$Q_{cnet} = Q_c + Q_{dir} + Q_{dif} + Q_{ref} + Q_{rg} + Q_{rv} + Q_{rs} + Q_{rains} + Q_{raine} + Q_{cond} \qquad (10.A37)$$

Heat flows: plastron (in contact with ground)

Due to its surface profile, part of the tortoise's plastron is considered to be in contact with the ground; the remainder has an air gap between its underside and the ground.

In this case, to solve the conduction equation for the plastron-ground system, the plastron and ground are divided into slices of equal thickness: 10 for the plastron and 1000 for the ground. The temperature of the first slice of the plastron (adjacent to the tortoise internals) is assumed to be at the same temperature as the internals; the 1000th slice of the ground is assumed to remain at the long-term average ambient temperature.

The portion of the plastron in contact with the gut receives heat from the gut according to the temperature gradient between the first two slices of the plastron. The heat flow into the plastron is therefore given by the standard heat conduction equation:

$$Q_{pc} = A_{spl}(PC) \cdot k_1 \cdot \frac{\left(T_{2gc,1} - T_{2gc,2}\right)}{dz} \qquad (10.A38)$$

where A_{spl} the surface area of the entire plastron (m^2); dz the thickness of each slice of plastron or ground (set equal to 10% of plastron thickness) (m); *PC* the fraction of plastron in direct contact with ground; Q_{pc} the heat rate to plastron (in contact with the ground) by conduction from the gut (W); $T_{2gc,1}$ the temperature of the first slice of the plastron-ground system (adjacent to the internals (°C); and $T_{2gc,2}$ the temperature of the second slice of the plastron-ground system (°C).

An initial temperature profile is set for the 1010 slices of the plastron-ground system, which gives the solution for Q_{pc} in the first time step. Solution of the 1-D conduction equation to calculate the temperature profile at subsequent time steps is carried out using a standard difference method.

Heat flows: plastron (not in contact with ground)

There are three mechanisms of heat transfer between the ground and that part of the plastron not in direct contact with the ground:

1. conduction of heat from ground to plastron via the air gap,
2. radiation exchange between the ground under tortoise and the plastron, and
3. conduction of heat into plastron from internals (temperature gradient across plastron).

Convective heat transfer is neglected as the air gap is small and unlikely to support significant convective currents.

Preliminary considerations

If the tortoise is considered "active," then the thickness of the air gap is assumed to be greater than if the tortoise is "inactive" and the surface temperature of the ground under the plastron is assumed to be the surface temperature of open ground (as the tortoise is assumed to be moving over the ground).

If the tortoise is "inactive," then the tortoise is not moving and surface temperature of the ground under the plastron is calculated in a similar way to that described by Eq. (10.A38).

Conduction through air gap

Conduction from the ground via the air gap to the plastron is given by:

$$Q_{pcag} = A_{spl}(1 - PC)\cdot k_{ag}\cdot \frac{\left(T_{2ag} - T_p\right)}{x_{ap}} \qquad (10.A39)$$

where k_{ag} is the thermal conductivity of air in air gap (at the average temperature between ground and plastron) (W/m K). Thermal conductivity of air is linear with temperature. Q_{pcag} is the heat rate to plastron (not in contact with the ground) by conduction from the ground through the air gap (W); T_{2ag} the temperature of the ground under the plastron (not in contact with the ground) (°C). If the tortoise is "active" this is taken as the surface temperature of open ground. T_p is the temperature of the exterior of the plastron (°C); x_{ap} the thickness of the air gap under the plastron (m). This takes different values according whether the tortoise is "active" or not.

Thermal radiation between ground and plastron

As the air gap is relatively thin and perhaps enclosed by sections of the plastron in direct contact with the ground, the air-gap enclosure between the ground and plastron is assumed to be a "black-body enclosure." In this case, all emissivities and view factors are equal to 1. The heat rate between ground and plastron is therefore given by the Stefan−Boltzmann equation:

$$Q_{prag} = \sigma A_{spl}(1 - PC)\cdot\left(T_{2ag}^4 - T_p^4\right) \qquad (10.A40)$$

where Q_{prag} is the heat rate into plastron due to thermal radiation from ground (W).

All temperatures in this case are in Kelvin.

Conduction between tortoise internals and plastron

The heat flowing through the plastron due to the temperature driving force between plastron exterior and internal temperature must also be considered. The heat rate into the plastron is given by the conduction equation:

$$Q_{pcond} = \frac{A_{spl}(1 - PC)k_1(T_i - T_p)}{x_p} \qquad (10.A41)$$

where Q_{pcond} is the heat rate into carapace due to conduction (W) and x_p is the thickness of plastron (m).

Net heat rate into plastron (not in direct contact with ground)

The net heat rate into the section of the plastron not in direct contact with the ground (Q_{panet}) is calculated by summing the heat rates from the previous three subsections.

$$Q_{panet} = Q_{pcag} + Q_{prag} + Q_{pcond} \qquad (10.A42)$$

Heat flows: internal

There are six mechanisms of heat transfer into the tortoise internals:

1. metabolism,
2. sensible heat gain by respiration,
3. gain of latent heat of evaporation due to respiration (almost always a heat loss, so value is negative),
4. conduction from carapace ($= -Q_{condc}$),
5. conduction from plastron area in contact with ground ($= -Q_{pc}$), and
6. conduction from plastron area not in contact with ground ($= -Q_{pcond}$).

Each mechanism is presented in the following subsections.

Metabolism

Heat is generated within the tortoise by metabolism. The heat generated depends on the mass and activity of the tortoise, and its internal temperature.

Heat generated by metabolism is assumed to be given by the following equations (Andrews and Pough 1985):

$$O_{2s} = 3.61 \times 10^{-6} M_t^{0.80}\, 10^{(0.038\, T_i)}\, 10^{(0.14\, Act)} \qquad (10.A43)$$

$$Q_m = O_{2s}\cdot MCF \qquad (10.A44)$$

where O_{2s} is the rate of metabolized oxygen (mL/s); T_i the internal gut temperature of tortoise (°C); Act the metabolic state of tortoise (as listed in Andrews and Pough (1985), (0 = "standard"; 1 = "resting"). In this report, these values are taken to be 0 = inactive; 1 = active; MCF the metabolic conversion factor = 20.1 J/mL O_2 metabolized; Q_m the heat rate to tortoise by metabolism (W); and M_t the mass of tortoise (g in this equation only).

Respiration

Preliminary data

A breathing rate must be determined to calculate all heat flows associated with respiration.

An estimate of air breathing rate can be made from the rate of oxygen metabolized (see earlier) and an assumption on the volume of oxygen in exhaled air (about 16% in humans from 20.9% in air).

$$\dot{V} = \frac{10^{-6}O_{2s}}{(20.9\% - O_{2ex})} \qquad (10.A45)$$

where $\dot{V}$ is the respiration rate (m^3/s) and O_{2ex} the percentage of oxygen in exhaled breath.

Sensible heat

Heat rate (W) into the tortoise due to the change in sensible heat of inhaled and exhaled air is given by the following equation:

$$Q_s = \rho_a \dot{V} C_{pa}(T_a - T_i) \tag{10.A46}$$

where C_{pa} is the specific heat capacity of ambient air (J/kg K); Q_s the sensible heat rate to tortoise by respiration (W); T_a the ambient temperature (°C); T_i the internal temperature of tortoise (°C); and ρ_a the density of ambient air (kg/m^3).

Latent heat

The heat rate to the tortoise is given by the difference in water content in inhaled and exhaled breath, and the latent heat of water. The water content of saturated air (in kg/m^3) as a function of temperature (at ambient pressure) is calculated using the Antoine equation and the perfect gas law.

The increase in water content of the exhaled breath compared with that inhaled is:

$$\Delta c_w = c_w|_{T_i} - c_w|_{T_a} \cdot (RH) \tag{10.A47}$$

The heat flow into the tortoise due to latent heat in respiration is given by the following equation:

$$Q_l = -\Delta c_w \bar{V} L_w \tag{10.A48}$$

where Q_l is the heat rate to tortoise by latent heat (W); c_w the water content of saturated air, which is a function of air temperature (kg/m^3); RH the relative humidity; and L_w the latent heat of water (J/kg).

Net heat rate into internal tissue mass

The net heat rate into the tortoise internals (Q_{inet}) is calculated by summing the heat rates from the previous subsections.

$$Q_{inet} = Q_m + Q_s + Q_l - Q_{condc} - Q_{pcond} - Q_{pc} \tag{10.A49}$$

Heat flows: open ground adjacent to tortoise

Very similar methods are used to specify heat flows to the first slice of open ground as are used for the carapace. However, there are some differences, mostly due to geometry. The description is abbreviated to highlight any differences. The following heat flows are assessed:

1. convection,
2. direct solar radiation,
3. diffuse solar radiation,
4. thermal radiation between carapace and open ground,
5. thermal radiation between surrounding terrestrial environment and open ground,
6. thermal radiation between sky and open ground,
7. sensible heat transfer due to rain falling on open ground,
8. latent heat by evaporation of rain film from open ground, and
9. conduction of heat into first slice of open ground from depth of ground (temperature gradient at ground surface).

Each is specified in the following subsections. In this case, all heat flows are per unit area of ground.

Convection

The HTC for forced convection over flat open is modeled using the *j*-factor analogy (in Bird *et al.* 1960: Fig. 13.2-3 therein) which plots j_H against Re). The dotted line in this figure is used for the average *j*-factor over a cumulative distance [in this case 2 (rv): the diameter of the vegetation cylinder] and a quartic data fit is used to relate the logarithm of j_H to that of Re (discussed next).

The HTC and subsequently the heat flux into the tortoise by forced convection over the carapace is calculated by the following equations.

Values for physical properties of air are taken at the average film temperature (between the open ground and ambient temperature).

$$Re = \frac{\rho_f u d}{\mu_f} \tag{10.A50}$$

$$j_H = \text{alog}_{10}\left[-177.57 + 97.495 \log_{10}(Re) - 20.347(\log_{10}(Re))^2 + 1.8843(\log_{10}(Re))^3 - 0.0654(\log_{10}(Re))^4\right] \tag{10.A51}$$

$$Pr = \frac{C_{pa}\,\mu_f}{k_f} \tag{10.A52}$$

$$Nu = j_H Re\, Pr^{1/3} \tag{10.A53}$$

$$h = \frac{Nuk_f}{d} \tag{10.A54}$$

$$Q_{2conv} = h(T_a - T_2) \tag{10.A55}$$

where C_{pa} is the specific heat capacity of air in film (J/kg K). There is little variation of this with temperature, so $C_{pf} = C_{pa} = 1005$ J/kg K. d is the characteristic length of open ground (m). In this case the dimension is $2 \times (rv)$, in which (rv) is the distance from the tortoise to the vegetation; h the HTC over open ground (W/m^2 K); j_H the *j*-factor for heat transfer (dimensionless); k_f the thermal conductivity of air in film

(W/m K). Calculated at a given temperature by a linear regression of data in West (1981); Nu is the Nusselt number (dimensionless); Pr the Prandtl number (dimensionless); Q_{2conv} the heat rate into first slice of open ground forced convection (W); Re the Reynolds number (dimensionless); T_2 the open ground surface temperature (°C); T_a the ambient temperature (°C); u the wind speed (m/s); μ_f the dynamic viscosity of air in film (kg/m s); and ρ_f the density of air in film (kg/m^3) calculated by the perfect gas law.

Direct solar radiation

The heat rate to a unit area of horizontal, open ground is given by:

$$Q_{2dir} = a_2 I^*_{DH} \tag{10.A56}$$

where a_2 is the absorptivity of ground to solar radiation (dimensionless); I^*_{DH} the direct solar radiation flux (under clear or cloudy skies) to the horizontal plane (W/m^2), see Eq. (10.A10); and Q_{2dir} the heat rate to unit area of surface of open ground by direct solar radiation (W).

In the present model the open ground is considered to be surrounded by vegetation (of user-stated dimensions and a user-defined height. If the sun has not risen above the top of the vegetation, then Q_{2dir} is set to zero.

Diffuse solar radiation

The heat rate to the first slice of open ground (on a per unit area basis) is given by

$$Q_{2dif} = a_2 I^*_{dH} \frac{F_{24}}{1.0} \tag{10.A57}$$

where I^*_{dH} is the diffuse solar radiation flux (under clear or cloudy skies) to horizontal ground (W/m^2), see Eq. (10.A11); Q_{2dif} the heat rate to open ground (per unit area) by diffuse solar radiation (W); and F_{24} the view factor for radiation from ground (surface 2) to sky (surface 4) (dimensionless).

The adjustment on flux by the factor $F_{24}/1.0$ accounts for the portion of the sky obscured by vegetation. For no vegetation present at all, the maximum value of F_{24} is 1; therefore the diffuse solar flux reaching the ground with surrounding vegetation is scaled accordingly.

Thermal radiation between ground and carapace

Net radiative heat transfer into a unit area of open ground from the carapace is governed according to the following equation. This is the same quantity of net heat as emitted from the carapace to the ground (Eq. 10.A23) but adjusted to a unit area basis.

$$Q_{2rc} = \frac{-Q_{rg}}{\pi\left[(rv)^2 - r_t^2\right]} \tag{10.A58}$$

where Q_{2rc} is the heat rate to unit area of open ground due to radiation exchange with carapace (W); rv the radius of open ground in which the tortoise is situated (m); and r_t the radius of tortoise (m).

Thermal radiation between ground and terrestrial environment

Radiative heat transfer between the open ground and the surrounding vegetative environment is governed according to the following equation:

$$Q_{2rv} = \sigma F_{23}\left(e_3 T_3^4 - e_2 T_2^4\right) \tag{10.A59}$$

where e_2 is the emissivity of open ground surrounding tortoise (dimensionless); e_3 the emissivity of vegetation surrounding tortoise (dimensionless); F_{23} the view factor between open ground and the vegetation (dimensionless); Q_{2rv} the heat rate per unit area to open ground due to radiative exchange with surrounding vegetation (W); T_2 the surface temperature of open ground (K); and T_3 the temperature of environment surrounding tortoise (K), which is assumed to be at ambient temperature (T_a).

Thermal radiation between ground and sky

Radiative heat transfer (per unit area) between the first slice of open ground and the sky is governed according to the following equation:

$$Q_{2rs} = \sigma F_{24}\left(e_4 T_4^4 - e_2 T_2^4\right) \tag{10.A60}$$

where e_4 is the emissivity of the sky (dimensionless); F_{24} the view factor between open ground and the sky (dimensionless); Q_{2rs} the heat rate (per unit area) to open ground due to radiation from the sky (W); and T_4 the temperature of sky (K).

Sensible heat transfer to open ground due to rainfall

Heat is transferred to (or more likely away from) the open ground by rain falling on its surface. If the rain film on the surface quickly reaches ground temperature, then the rate of heat transfer per unit area to the open ground is given by:

$$Q_{2rains} = \rho_w F_t C_{pw} (T_{rain} - T_2)$$

where Q_{2rains} is the sensible heat rate to open ground per unit area from falling rain film (W); ρ_w the density of water (1000 kg/m^3); F_t the rainfall rate to unit area of

open ground (m^3/s); C_{pw} the specific heat capacity of water (4186 J/kg K); and T_{rain} the temperature of rain (°C).

Latent heat due to evaporation of rain

The evaporation rate per unit area from the surface of the rain film on open ground can be predicted using the Chilton–Colburn (or *j*-factor) analogy between heat, mass, and momentum transfer.

Water is evaporated due to the differential in vapor pressure (or mole fraction) between the air–water interface at the rain layer on the ground surface (which is assumed saturated at the ground surface temperature) and the bulk air. The procedure is the same as for the water evaporating from the carapace except the characteristic length for the Reynolds number is twice the distance between the tortoise and the vegetation and the equation to give a value of the Schmidt number is given by equation 21.2-25 in Bird *et al.* (1960).

$$j_M = j_H \tag{10.A61}$$

where j_H is calculated from Eq. (10.A51), and

$$Sh = j_M\, Re\, Sc^{1/3} \tag{10.A62}$$

And the heat into the ground is calculated as for Eq. (10.A35):

$$Q_{2raine} = -L_w.\dot{M} \tag{10.A63}$$

where Re is the Reynolds number (dimensionless); Sc the Schmidt number (dimensionless); Sh the Sherwood number (dimensionless); L_w the latent heat of evaporation of water (roughly constant at all temperatures considered 2.43×10^{-6} J/kg); Q_{2raine} the heat rate into the open ground by evaporation of water from its surface (W); and $\dot{M}$ the mass rate of water evaporating from surface of open ground (kg/s).

Conduction into first slice of open ground

The heat flowing into the first slice of open ground from the second slice is given on a per unit area basis by:

$$Q_{2cond} = \frac{k_2\left(T_{2g(2,2)} - T_{2g(2,1)}\right)}{dz} \tag{10.A64}$$

where dz is the thickness of slices of ground (m); k_2 the thermal conductivity of open ground (W/m K). There are two potential values for wet and dry conditions. Both specified by the user. Q_{2cond} is the heat rate per unit area into first slice of open ground from second due to conduction (W); $T_{2g(2,1)}$ the temperature of first slice of open ground (°C); and $T_{2g(2,2)}$ the temperature of second slice of open ground (°C).

Net heat rate into first slice of open ground

The net heat rate (Q_{2net}) into the first slice of open ground (thickness dz) is calculated by summing the heat rates from the previous subsections.

$$Q_{2net} = Q_{2conv} + Q_{2dir} + Q_{2dif} + Q_{2rc} + Q_{2rv} + Q_{2rs} + Q_{2rains} + Q_{2raine} + Q_{2cond} \tag{10.A65}$$

Solution and integration of heat balances

Each of the heat balances in section is integrated numerically over a small time step and the temperatures of each component are then updated. The heat balances are not considered in the same order.

Heat balance: open ground

The heat balance to the first slice of open ground is solved over time step dt.

The term $T_{2\,(i,\ j)}$ refers to the ground temperature at time step i and distance step j into ground.

$$H_{2net} = Q_{2net} \cdot dt \tag{10.A66}$$

$$\Delta T_2 = \frac{H_{2net}}{dz \cdot \rho_2 \cdot C_{p2}} \tag{10.A67}$$

$$T_{2(i+1,1)} = T_{2(i,1)} + \Delta T_2 \tag{10.A68}$$

where C_{p2} is the specific heat capacity of open ground (J/kg K). Value for both wet and dry ground are used. dt is the time step (s); dz the thickness of slices of open ground (m); H_{2net} the net heat into first slice of open ground (per unit area) during time step dt (J); Q_{2net} the net heat rate into open ground (per unit area) (W); $T_{2(i,1)}$ the temperature of first slice of open ground for ith time step (°C); $T_{2(i+1,1)}$ the temperature of first slice of open ground for $(i+1)$th second time step (°C); ΔT_2 the change in temperature of open ground over time step (°C); and ρ_2 the density of open ground (kg/m^3).

The general 1-D conduction equation for this situation is:

$$\frac{\partial T}{\partial z} = \alpha \frac{\partial^2 T}{\partial z^2} \tag{10.A69}$$

where T is the temperature (°C); z the distance into ground (m); and α the thermal diffusivity of ground (m^2/s); and $\alpha = k/(\rho \cdot C_p)$.

Given an initial temperature profile for all z, and two boundary conditions (T at $z = 0$ and also at large z), this partial differential equation can be solved numerically by the following scheme:

$$T_{i+1,j} = r \cdot T_{i,j+1} + (1 - 2r) \cdot T_{i,\,j} + r \cdot T_{i,j-1} \tag{10.A70}$$

$$r = \alpha \frac{(dt)}{(dz)^2} \tag{10.A71}$$

where r is the stability parameter (dimensionless). The value of r must be less than 0.5 for numerical stability of solving scheme. $T_{i,j}$ is the temperature for ith time step and jth distance step (°C).

In the case of open ground, T_2 is used as above and α varies with distance into the ground between wet ground and dry ground values according to the depth of rainfall penetration.

At all time steps and at each value of z, if the net cumulative volume of rain that has soaked into the ground per unit area (total volume of rain fallen minus total evaporated) is less than the product of z and ground voidage (space available for flow of fluids), then the value of α used is that of dry conditions, otherwise the "wet" value is used.

1000 distance steps are used.

For each time step the initial and boundary conditions are:

$T_{i,j}$ (for $j = 1-999$): initial temperature profile set by user, then recalculated at each time step

$T_{i,1000}$: average long-term ambient temperature (held constant for all i)

$T_{i+1,1}$: temperature of the ground surface at next time step

The distance step is taken as 10% of the plastron thickness.

The time step is adjusted so that r is always 0.45 to allow some leeway on solution stability (for the maximum value of α: wet or dry).

The expression discussed earlier for $T_{i+1,j}$ is then marched through for $j = 2-999$.

Heat balance: internal

The heat balance for the tortoise internals is solved over time step dt.

$$H_{inet} = Q_{inet} \cdot dt \tag{10.A72}$$

$$\Delta T_i = \frac{H_{inet}}{M_i \cdot C_{p2}} \tag{10.A73}$$

$$T_{i,\,next\ time\ step} = T_i + \Delta T_i \tag{10.A74}$$

where C_{pi} is the specific heat capacity of tortoise internals (J/kg K); dt the time step (s); H_{inet} the net heat into tortoise internals during time step dt (J); M_i the mass of tortoise internals (kg); Q_{inet} the net heat rate into tortoise internals (W); T_i the temperature of tortoise internals during time step considered (°C); $T_{i\ next\ time\ step}$ the temperature of tortoise internals at start of next time step (°C); and ΔT_i the change in temperature of tortoise internals over time step (°C).

Heat balance: carapace

The heat balance for the tortoise carapace is solved over time step dt.

$$H_{cnet} = Q_{cnet} \cdot dt \tag{10.A75}$$

$$\Delta T_{1,\,av} = \frac{H_{cnet}}{M_c \cdot C_{p1}} \tag{10.A76}$$

$$T_{1,\,av,\,next\ time\ step} = \frac{T_1 + T_i}{2} + \Delta T_{1,\,av} \tag{10.A77}$$

$$T_{1,\,next\ time\ step} = 2\,T_{1,\,av,\,next\ time\ step} - T_{i,\,next\ time\ step} \tag{10.A78}$$

where C_{p1} is the specific heat capacity of carapace (J/kg K); dt the time step (s); H_{cnet} the net heat into carapace during time step dt (J); M_c the mass of carapace (kg); Q_{cnet} the net heat rate into carapace (W); $\Delta T_{1,av}$ the change in average temperature of carapace during time step considered (°C); $T_{1,\,av,\,next\ time\ step}$ the average temperature of carapace at start of next time step (°C); and $T_{1,\,next\ time\ step}$ the surface temperature of carapace at start of next time step (°C).

Heat balance: plastron (not in contact with ground)

The heat balance for the tortoise plastron not in contact with the ground is solved over time step dt.

$$H_{panet} = Q_{panet} \cdot dt \tag{10.A79}$$

$$\Delta T_{p,\,av} = \frac{H_{panet}}{M_p \cdot (1 - PC) \cdot C_{p1}} \tag{10.A80}$$

$$T_{p,\,av,\,next\ time\ step} = \frac{T_p + T_i}{2} + \Delta T_{p,\,av} \tag{10.A81}$$

$$T_{p,\,next\ time\ step} = 2\,T_{p,\,av,\,next\ time\ step} - T_{i,\,next\ time\ step} \tag{10.A82}$$

where C_{p1} is the specific heat capacity of carapace (J/kg K); dt the time step (s); H_{panet} the net heat into plastron (not in contact with ground) carapace during time step dt (J); M_p the total mass of plastron (kg); Q_{panet} the net heat rate into plastron (not in contact with ground) (W); $\Delta T_{p,av}$ the change in average temperature of plastron (not in contact with ground) during time step considered (°C); $T_{p,\,av,\,next\ time\ step}$ the average temperature of plastron (not in contact with ground) at start of next time step (°C); $T_{p,\,next\ time\ step}$ the surface temperature of plastron (not in co tact with ground) at start of next time step (°C).

Heat balance: plastron (in contact with ground) and ground beneath

The heat balance for the tortoise plastron (not in contact with the ground) and the ground beneath is solved as one system over a time step dt in an equivalent manner to that of the open ground. However, in this case, the number of distance steps is 1010 (10 for the plastron and 1000 for the ground).

The general 1-D conduction equation for this situation is:

$$\frac{\partial T}{\partial z} = \alpha \frac{\partial^2 T}{\partial z^2} \quad (10.A83)$$

where T is the temperature (°C); z the distance into system (m); and α the thermal diffusivity of system (m^2/s). $\alpha = k/(\rho \cdot C_p)$.

Given an initial temperature profile for all z, and two boundary conditions (T at $z = 0$ and also at large z), this partial differential equation can be solved numerically by the following scheme:

$$T_{i+1,j} = r \cdot T_{i,j+1} + (1 - 2r) \cdot T_{i,j} + r \cdot T_{i,j-1} \quad (10.A84)$$

$$r = \alpha \frac{(dt)}{(dz)^2} \quad (10.A85)$$

where r is the stability parameter (dimensionless). The value of r must be less than 0.5 for numerical stability of solving scheme. r takes on different values for plastron and ground (depending on the thermal diffusivity (α) of each component): r_p for $j = 1-10$ and $r_{g,dry}$ for $j = 11-1010$. $T_{i,j}$ is the temperature for ith time step and jth distance step (°C).

For each time step the initial and boundary conditions are:

$T_{i,j}$ (for $j = 1-1009$): initial temperature profile set by user, then recalculated at each time step

$T_{i,1010}$: average long-term ambient temperature (held constant for all i)

$T_{i+1,1}$: internal tortoise temperature at next time step ($T_{i,\ next\ time\ step}$)

The distance step is taken as 10% of the plastron thickness.

The expression discussed earlier for $T_{i+1,j}$ is then iterated for $j = 2-1009$.

Heat balance: ground under plastron (not in contact with ground)

The heat balance to the first slice of ground under the plastron (not in contact with the ground) is solved over time step dt.

The term $T_{2gnc(i,\ j)}$ refers to the ground temperature at time step i and distance step j into ground.

$$H_{2ncnet} = Q_{2ncnet} \cdot dt \quad (10.A86)$$

$$\Delta T_{2gnc} = \frac{H_{2ncnet}}{A_{spl}(1 - PC)\, dz \cdot \rho_2 \cdot C_{p2}} \quad (10.A87)$$

$$T_{2gnc\ (i+1,1)} = T_{2gnc(i,1)} + \Delta T_{2gnc} \quad (10.A88)$$

where C_{p2} is the specific heat capacity of ground (J/kg K). The dry value is used. dt is the time step (s); dz the thickness of slices of ground (m); H_{2ncnet} the net heat into first slice of ground under plastron (not in contact with ground) during time step dt (J); Q_{2ncnet} the net heat rate into ground under plastron (not in contact with ground) (W); $T_{2gnc\ (i,\ 1)}$ the temperature of first slice of ground for ith time step (°C); $T_{2gnc\ (i+1,1)}$ the temperature of first slice of ground for $(i + 1)$th second time step (°C); ΔT_{2gnc} the change in temperature of first slice of ground over time step (°C); and ρ_2 the density of ground (kg/m^3). Dry value used.

The general 1-D conduction equation for this situation is:

$$\frac{\partial T}{\partial z} = \alpha \frac{\partial^2 T}{\partial z^2} \quad (10.A89)$$

where T is the temperature (°C); z the distance into ground (m); and α the thermal diffusivity of ground (m^2/s). $\alpha = k/(\rho \cdot C_p)$.

Given an initial temperature profile for all z, and two boundary conditions (T at $z = 0$ and also at large z), this partial differential equation can be solved numerically by the following scheme:

$$T_{i+1,\ j} = r \cdot T_{i,\ j+1} + (1 - 2r) \cdot T_{i,\ j} + r \cdot T_{i,\ j-1} \quad (10.A90)$$

$$r = \alpha \frac{(dt)}{(dz)^2} \quad (10.A91)$$

where r is the stability parameter (dimensionless). The value of r must be less than 0.5 for numerical stability of solving scheme. $T_{i,\ j}$ the temperature for ith time step and jth distance step (°C).

In the case of ground under the plastron (not in contact with the ground), T_{2gnc} is used as earlier.

1000 distance steps are used.

For each time step the initial and boundary conditions are:

$T_{i,j}$ (for $j = 1-999$): initial temperature profile set by user, then recalculated at each time step

$T_{i,\ 1000}$: average long-term ambient temperature (held constant for all i)

$T_{i+1,1}$: third expression of this section (discussed earlier)

The distance step is taken as 10% of the plastron thickness.

The expression discussed earlier for $T_{i+1,j}$ is then iterated for $j = 2-999$.

Relative importance of input variables for core temperature

To determine the influence of each input variable on the tortoise internal temperature, a series of model runs were performed varying each parameter in turn. The minimum and maximum internal temperatures (minimum and maximum T_b, respectively) for each run were compared against

that for a standard scenario. Objective comparison of influence of the different input parameters on internal temperature is difficult, because some parameters are continuous variables, whereas others are discrete (e.g., tortoise in open or shade). Therefore the comparison method used was semiquantitative in that physically plausible changes (both positive and negative) were made to each input parameter and the change in internal temperature recorded. Over some 80 runs used in this parametric survey, the 20 parameters that generated the greatest change to internal temperature were considered to be of "high" influence; the 20 generating least change were classified as "low" influence; all others were considered of medium influence (Table 10.A1). Input variables were divided into extrinsic (environmental factors) and intrinsic (based on properties of the tortoise). The extrinsic factors that were most important in determining tortoise core temperature included ambient maximum and minimum temperatures (upon which the solar radiation and sinusoidal ambient temperature projections through the day were based), rainfall, cloud cover, distance to vegetation and vegetation height, and cover/noncover. Wind speed, humidity, cloud type, and clearness of the sky all had medium impacts. Properties of the ground and vegetation had medium or low impact, except for the emissivity of vegetation, which had a high impact on minimum T_b. In general, intrinsic factors were less important determinants of tortoise core temperature than extrinsic ones. Indeed, of the 18 input variables considered (see Table 10.A1), only 3 (emissivity of carapace and plastron, tortoise activity, and radius) had large effects on either minimum T_b, minimum T_b, or both.

TABLE 10.A1 The relative importance of model input variables on maximum T_b, and minimum T_b internal tortoise temperatures.

Parameter	Influence on maximum T_b	Influence on minimum T_b
Extrinsic factors		
Maximum ambient temperature	H	H
Minimum ambient temperature	H	H
Cloud cover	H	H
Rainfall	H	H
Distance to vegetation	H	H
Tortoise in open or under cover	H	H
Emissivity of vegetation	M	H
Height of vegetation	H	M
Wind speed	M	M
Relative humidity	M	M
Cloud type	M	M
Clearness of sky	M	M
Emissivity of ground	M	M
Emissivity of water film on carapace (when raining)	M	M
Absorptivity of ground to solar radiation	M	M
Density of ground	L	L
Thermal conductivity of ground	L	L
Specific heat capacity of ground	L	L
Sensitivity of view factors	L	L
Intrinsic factors		
Emissivity of carapace and plastron	H	H

(*Continued*)

TABLE 10.A1 (Continued)

Parameter	Influence on maximum T_b	Influence on minimum T_b
Radius of tortoise	M	H
Tortoise activity (active or basal metabolism)	H	M
Absorptivity of carapace to solar radiation	H	M
Thickness of carapace	M	M
Carapace and plastron thermal conductivity	M	M
Density of tortoise internals	M	M
Specific heat capacity of tortoise internals	M	M
Ratio of active to basal metabolism	M	M
Ratio of convective heat transfer coefficient (hemisphere/sphere)	M	M
Carapace and plastron density	L	M
Carapace and plastron specific heat capacity	M	L
Thickness of air gap under plastron (active tortoise)	L	M
Thickness of plastron	L	L
Percentage of plastron in contact with ground (passive tortoise)	L	L
Thickness of air gap under plastron (passive tortoise)	L	L
Variable partitioning of blood flow through body from core to periphery	L	L

References

Andrews, R. M., and F. H. Pough. 1985. Metabolism of squamate reptiles: allometric and ecological relationships. *Physiological Zoology* **58**:214–231.

Angilletta, M. J. 2001. Thermal and physiological constraints on energy assimilation in a widespread lizard (*Sceloporus undulatus*). *Ecology* **82**:3044–3056.

Angilletta, M. 2009. Thermal adaptation: a theoretical and empirical synthesis. Oxford University Press, Oxford, United Kingdom.

Bakken, G. S. 1976. A heat transfer analysis of animals: unifying concepts and the application of metabolism chamber data to field ecology. *Journal of Theoretical Biology* **60**(2):337–384.

Bastille-Rousseau, G., C. B. Yackulic, J. P. Gibbs, J. L. Frair, F. Cabrera, and S. Blake. 2019. Migration triggers in a large herbivore: Galápagos giant tortoises navigating resource gradients on volcanoes. *Ecology* **100**:e02658.

Bathiany, S., V. Dakos, M. Scheffer, and T. M. Lenton. 2018. Climate models predict increasing temperature variability in poor countries. *Science Advances* **4**:eaar5809.

Bird, R. B., E. S. Stewart, and E. N. Lightfoot. 1960. Transport phenomena. Second Edition. John Wiley & Sons, New York, USA.

Blake, S., C. B. Yackulic, F. Cabrera, W. Tapia, J. P. Gibbs, F. Kummeth, and M. Wikelski. 2013. Vegetation dynamics drive segregation by body size in Galapagos tortoises migrating across altitudinal gradients. *Journal of Animal Ecology* **82**:310–321.

Cayot, L. J. 1987. Ecology of giant tortoises (*Geochelone elephantopus*) in the Galápagos Islands. Syracuse University, New York, USA.

Colinvaux, P. A. 1984. The Galápagos climate: present and past. In R. Perry, editor. Key environments: Galápagos. Pergamon Press, Oxford, United Kingdom.

Conroy, J. L., A. Restrepo, J. T. Overpeck, M. Steinitz-Kannan, J. E. Cole, M. B. Bush, and P. A. Colinvaux. 2008. Unprecedented recent warming of surface temperatures in the eastern tropical Pacific Ocean. *Nature Geoscience* **2**:46–50.

Falcón, W., R. P. Baxter, S. Furrer, M. Bauert, J. M. Hatt, G. Schaepman-Strub, A. Ozgul, N. Bunbury, M. Clauss, and D. M. Hansen. 2018. Patterns of activity and body temperature of Aldabra giant tortoises in relation to environmental temperature. *Ecology and Evolution* **8**:2108–2121.

Fei, T., A. K. Skidmore, V. Venus, T. J. Wang, M. Schlerf, B. Toxopeus, S. van Overjijk, M. Bian, and Y. L. Liu. 2012. A body temperature model for lizards as estimated from the thermal environment. *Journal of Thermal Biology* **37**:56–64.

Fischer, J., and D. B. Lindenmayer. 2007. Landscape modification and habitat fragmentation: a synthesis. *Global Ecology and Biogeography* **16**:265–280.

Fritts, T. H. 1984. Evolutionary divergence of giant tortoises in Galapagos. *Biological Journal of the Linnean Society* **21**:165–176.

Harlow, H. J., D. Purwandana, T. S. Jessop, and J. A. Phillips. 2010. Body temperature and thermoregulation of Komodo dragons in the field. *Journal of Thermal Biology* **35**:338–347.

Hoegh-Guldberg, O., D. Jacob, M. Taylor, and G. Zhou. 2019. The human imperative of stabilizing global climate change at 1.5°C. *Science* **365**:eaaw6974.

Howell, J. R. 2019. A catalogue of radiation heat transfer configuration factors. University of Texas at Austin.

Ihlow, F., J. Dambach, J. O. Engler, M. Flecks, T. Hartmann, S. Nekum, H. Rajaei, and D. Roedder. 2012. On the brink of extinction? How climate change may affect global chelonian species richness and distribution. *Global Change Biology* **18**:1520−1530.

IPCC. 2014. Climate change 2014: synthesis report. Contribution of working groups I, II and III to the fifth Assessment report of the intergovernmental panel on climate change. IPCC, Geneva, Switzerland.

Kearney, M., R. Shine, and W. P. Porter. 2009. The potential for behavioral thermoregulation to buffer "cold-blooded" animals against climate warming. *Proceedings of the National Academy of Sciences of the United States of America* **106**:3835−3840.

Kearney, M. R., and W. P. Porter. 2017. NicheMapR − an R package for biophysical modelling: the microclimate model. *Ecography* **40**:664−674.

Khatun, K. 2018. Land use management in the Galapagos: a preliminary study on reducing the impacts of invasive plant species through sustainable agriculture and payment for ecosystem services. *Land Degradation and Development* **29**:3069−3076.

Liu, Y. Y., L. Xie, J. M. Morrison, and D. Kamykowski. 2013. Dynamic downscaling of the impact of climate change on the ocean circulation in the Galapagos Archipelago. *Advances in Meteorology* **2013**:<https://doi.org/10.1155/2013/837432>.

Nolan, C., J. T. Overpeck, J. R. M. Allen, and S. T. Jackson. 2018. Past and future global transformation of terrestrial ecosystems under climate change. *Science* **361**:920−923.

O'Connor, M. P. 1999. Physiological and ecological implications of a simple model of heating and cooling in reptiles. *Journal of Thermal Biology* **24**:113−136.

O'Connor, M. P. 2000. Extracting operative temperatures from temperatures of physical models with thermal inertia. *Journal of Thermal Biology* **25**:329−343.

O'Connor, M. P., L. C. Zimmerman, E. M. Dzialowski, and J. R. Spotila. 2000. Thick-walled physical models improve estimates of operative temperatures for moderate to large-sized reptiles. *Journal of Thermal Biology* **25**:293−304.

Restrepo, A., P. Colinvaux, M. Bush, A. Correa-Metrio, J. Conroy, M. R. Gardener, P. Jaramillo, M. Steinitz-Kannan, and J. Overpeck. 2012. Impacts of climate variability and human colonization on the vegetation of the Galápagos Islands. *Ecology* **93**:1853−1866.

Ricklefs, R. E., and M. Wikelski. 2002. The physiology/life-history nexus. *Trends in Ecology and Evolution* **17**:462−468.

Sachs, J., and S. N. Ladd. 2010. Climate and oceanography of the Galapagos in the 21st century: expected changes and research needs. *Galapagos Research* **67**:50−54.

Schindler, D. E., and R. Hilborn. 2015. Prediction, precaution, and policy under global change. *Science* **347**:953−954.

Shine, R. 2005. Life-history evolution in reptiles. *Annual Review of Ecology, Evolution, and Systematics* **36**:23−46.

Spotila, J. R., P. W. Lommen, G. S. Bakken, and D. M. Gates. 1973. A mathematical model for body temperatures of large reptiles: implications for dinosaur ecology. *The American Naturalist* **107**:391−404.

Swingland, I. R. 1977. Reproductive effort and life history strategy of the Aldabran giant tortoise. *Nature* **269**:402−404.

Swingland, I. R., and J. G. Frazier. 1980. The conflict between feeding and overheating in the Aldabran giant tortoise. In C. J. Amlaner, D. W. Macdonald, editors. A handbook on biotelemetry and radio tracking. Pergamon Press (Oxford, United Kingdom).

Swingland, I. R., P. M. North, A. Dennis, and M. J. Parker. 1989. Movement patterns and morphometrics in giant tortoises. *Journal of Animal Ecology* **58**:971−985.

Trueman, M., and N. d'Ozouville. 2010. Characterization of Galapagos terrestrial climate in the face of global climate change. *Galapagos Research* **67**:26−37.

Tuff, K. T., T. Tuff, and K. F. Davies. 2016. A framework for integrating thermal biology into fragmentation research. *Ecology Letters* **19**:361−374.

Turner, J. S., and C. R. Tracy. 1985. Body size and the control of heat exchange in alligators. *Journal of Thermal Biology* **10**:9−11.

Walsh, S. J., and C. F. Mena. 2016. Interactions of social, terrestrial, and marine sub-systems in the Galapagos Islands, Ecuador. *Proceedings of the National Academy of Sciences of the United States of America* **113**:14536−14543.

Wang, S. K. 2001. Handbook of air conditioning and refrigeration. Second Edition. McGraw-Hill, New York, USA.

Watson, J., M. Trueman, M. Tufet, S. Henderson, and R. Atkinson. 2010. Mapping terrestrial anthropogenic degradation on the inhabited islands of the Galapagos Archipelago. *Oryx* **44**:79−82.

West, R. C. 1981. Handbook of chemistry and physics, 62nd Edition, 1981−1982, CRC Press Inc, Boca Raton, USA.

Wikelski, M., and L. M. Romero. 2003. Body size, performance and fitness in Galapagos marine iguanas. *Integrative and Comparative Biology* **43**:376−386.

Yackulic, C. B., S. Blake, and G. Bastille-Rousseau. 2017. Benefits of the destinations, not costs of the journeys, shape partial migration patterns. *Journal of Animal Ecology* **86**:972−982.

Zelinka, M. D., T. A. Myers, D. T. McCoy, S. Po-Chedley, P. M. Caldwell, P. Ceppi, S. A. Klein, and K. E. Taylor. 2020. Causes of higher climate sensitivity in CMIP6 models. *Geophysical Research Letters* **47**:e2019GL085782.

Zimmerman, L. C., M. P. O'Connor, S. J. Bulova, J. R. Spotila, S. J. Kemp, and C. J. Salice. 1994. Thermal ecology of desert tortoises in the eastern Mojave Desert: seasonal patterns of operative and body temperatures, and microhabitat utilization. *Herpetological Monographs* **8**:45−59.